ANALYSIS OF THERMAL CONDUCTIVITY OF FERROFLUIDS

by

Radhames de Jesus Rodriguez Gutierrez

A thesis submitted in partial fulfillment of the requirements for the degree of

MASTER OF SCIENCES
in
MECHANICAL ENGINEERING

UNIVERSITY OF PUERTO RICO
MAYAGÜEZ CAMPUS
2007

Approved by:

_____	_____
Oscar Perales, PhD Member, Graduate Committee	Date
_____	_____
Ricky Valentin, PhD Member, Graduate Committee	Date
_____	_____
Gustavo Gutierrez, PhD President, Graduate Committee	Date
_____	_____
Marcelo Suarez, PhD Representative of Graduate Studies	Date
_____	_____
Paul Sundaram, PhD Chairperson of the Department	Date

ABSTRACT

In this thesis, a transient hot wire system capable to measure the thermal conductivity of fluids is designed and used to characterized different ferrofluids. For measurement purposes an electrical insulation is provided to the platinum wire, in order to obtain appropriate values of thermal conductivities of electrical conductive fluid. The influence of some important parameters on the thermal conductivity is studied. Two $Mn_xZn_{1-x}Fe_2O_4$ (a water-based and a hydrocarbon-based) ferrofluids are compared in order to analyze their thermal conductivity. For the produced water-based ferrofluid, a chemical co-precipitation method and a double layer surfactant technique are employed in the production of the ferrofluids. The effect of the particle diameter, base fluid, volumetric concentration "ϕ" and chemical composition in the effective thermal conductivity of the ferrofluids are tested. The coating effect of the wire in the outcome of the transient hot wire system is analyzed by solving numerically the heat equation for the line source case. An enhancement is found in the effective thermal conductivity of all the nanofluids analyzed.

RESUMEN

En esta tesis se diseño un sistema basado en el método del alambre caliente para medir la conductividad térmica de fluidos y caracterizar diferentes ferrofluidos. Una cobertura aislante se aplicó al alambre de platino para el proceso de medición, con el objetivo de obtener valores apropiados de la conductividad térmica en el caso de analizarse fluidos eléctricamente conductores. Se estudió la influencia de ciertos parámetros críticos en la conductividad térmica de los ferrofluidos. Dos ferrofluidos de $Mn_xZn_{1-x}Fe_2O_4$ (uno suspendido en base de agua y otro suspendido en un hidrocarburo) se compararon con el propósito de analizar su conductividad térmica. Para la fabricación de los fluidos fueron se empleó el método de co-precipitación y la técnica de doble recubrimiento de surfactante. Se investigaron los efectos del diámetro de partícula, del fluido base, la concentración volumétrica "ϕ" y la composición química en la conductividad térmica efectiva de los ferrofluidos. La solución numérica de la ecuación de calor para el caso de una línea con generación; se usó para analizar el efecto del recubrimiento del alambre en los resultados obtenidos por el método del alambre caliente. Se encontró un incremento en la conductividad térmica efectiva de todos los ferrofluidos analizados.

DEDICATION

To my lovely wife Vleidy for being my inspiration and my biggest treasure. To my father Radhames and my mother Danae for giving me the gift of live. To my brothers Sandy and Francis and my sister Yaritza. Thanks for being all my strength and motivation. To my niece Karen. I love you all.

ACKNOWLEDGEMENTS

I would like to thank my advisor Dr. Gustavo Gutierrez for all his honest and sincere counseling, help and commitment, through all my graduate studies. I am also very grateful to Dr. Oscar Perales and his nanomaterials investigation group for his help and disposition, especially for his advice in the materials science area.

I am grateful to the Mechanical Engineering Department, to the NASA Ideas program and to the DoD-HBCU program for their academic and financial support. I also would like to thank Andres Velazco, Yarilin Cedeño, and especially to my friend Erick Orlando Bermudez MSME for all their unconditional help.

I also would like to thank Dr. Ramón Vázquez Espinosa, Dean of Engineering, for his support and Pedro Velázquez for his unconditional help and collaboration in the thermal fluid Lab. Finally, I specially thank to my friends for their support and all the memories…

CONTENTS

LIST OF FIGURES

LIST OF TABLES

LIST OF NOMENCLATURE

A	Normal area
c	specific heat
C	Calibration constant
Cl	Chloride
Cu	Copper
d	Particle diameter
D	Crystallite size
EG	ethylene glycol
EI	Exponential integral
Fe	Iron
h	Nanolayer thickness
H	Hydrogen
I	Electrical current
$K\ or\ k$	Thermal Conductivity
K	Scherer's constant
K_B	Boltzmann constant
MG	Maxwell-Garnett model
Mn	Manganese
n	Empirical shape factor
Na	Sodium
O	Oxygen
Pr	Prandalt number
q	Power per unit length
$\dot{q}$	Volumetric heat generation
q''	Heat transfer per unit length per unit time
Q	Heat flux
Q'	Heat flux per unit length
r	Radius or radial axis
R	Contact thermal Resistance per unit length

R	Electric resistance
R_b	Interfacial thermal resistance
Re	Reynolds number
RTD	Resistance Temperature Detector
S	Thermal capacity
T	Temperature
t	Time
t'	Dummy variable
τ_b	Time required for the Brownian diffusion
τ_c	Time required for the effect of convection
v	Kinematic viscosity
x	Atomic ratio
XRD	X-ray diffraction
Zn	Zinc
α	Thermal diffusivity or nanoparticle Biot number
β	Integral breadth of reflection or Kapitza resistance
ϕ	Volumetric concentration
Φ	Effective volume
γ	Euler's constant
η	Viscosity
λ	Wavelength of radiation
θ	Angle
ρ	Density
Δ	Difference
Ψ	Particle sphericity

Subscripts

$( )_{avg}$	Average	$( )_{ly}$	Layer
$( )_c$	Critical	$( )_p$	Particle
$( )_{eff}$	Effective	$( )_x$	Atomic radio
$( )_f$	Fluid or base fluid	$( )_w$	Wire

1. INTRODUCTION

Thermal conductivity is the property of a material that indicates its ability to conduct heat. Thermal conductivity, "*k* ", expresses the heat flux that will flow through the material if a certain temperature gradient exists over the material. This is an important property in conduction and convective heat transfer since it explains how heat is transported into and throughout the material.

If the thermal conductivity of a solid is bigger than the conductivity of a fluid, suspending solid fine particles is expected to increase the thermal conductivity of a fluid. Improving the thermal conductivity will increase the heat transfer rate that this fluid can transport compared with conventional fluids. Numerous theoretical and experimental studies of suspensions containing solid particle, such as millimeter or micrometer-sized particles, have been conducted since Maxwell's theoretical work was published more than 100 years ago [1].

However, due to the large size and high density of the micrometer-sized particles, they have not been of interest for practical applications in heat transfer because of problems such as sedimentation, erosion, increasing of flow resistance and clogging. New advances in material technology has made possible to process and produce nanometer-size particles, with average crystallite size below 50 nm, which can overcome these problems. Fluids with nanoparticles suspended in them are called 'nanofluids', a term proposed by Steve Choi in 1995 [2].

Nanofluids offer exciting new possibilities to enhance heat transfer performance compared with pure liquids and can be considered to be the next-generation of heat transfer fluids.

The development of nanofluids is still hindered by several issues such as the disagreement between the results of different investigations and a poor characterization of suspensions. Because of these reasons and due to the lack of theoretical understanding of the mechanism involved in the thermal conductivity of nanofluids, empirical measurements were preferable to theoretical predictions, in order to determine the observed enhancement in thermal conductivity of these fluids.

The present work is focused on the implementation of the transient hot wire method to study the thermal conductivity of Mn-Zn ferrofluids in particular by determining the influence of different parameters on the effective thermal conductivity of such fluids.

1.1 Motivation

Both an increasing demand of cooling ultra high heat flux equipment and the unprecedented recently trend to the miniaturization are continuously challenging the heat transfer technology. The temperature control of systems and equipments is an important requirement in industries such transportation and electronics and in processes involving electronic chips, laser applications or similar high energy devices [3], where the thermal properties of the fluids play an important roll.

As a result, the development of more efficient cooling systems and the ability to offer new alternatives in heat management is a growing necessity today; this fact promotes several

research interests and studies. Among of then, the application of additives to liquids if often involved because conventional heat transfer fluids have poor heat transfer properties compared with most solids.

Suspended nanoparticles in various base fluids can alter the fluid flow and heat transfer characteristics of the base fluid, especially when metallic particles are used. There are many factors that can influence the thermal conductivity in nanofluids such as lattice structure of the nanoparticles and the base fluid, its density, temperature, electrical conductivity, concentration of nanoparticles, nanoparticle size and shape, type and concentration of the surfactant and dispersion method, for instance.

More studies need to be carried out in order to understand the contribution of all these parameters to the enhancement of the thermal conductivity of nanofluids. Successful use and understanding of nanofluids will support the current trend toward component miniaturization by enabling the design of smaller and lighter heat exchanger systems, because they exhibit unexpected properties specially a higher thermal conductivity [4, 5], replacing in this way conventional fluids.

1.2 Objectives and Tasks

Main Objective

Study the influence of some important parameters, such as the thermal conductivity of the base fluid, the particle diameter, the volumetric concentration and the chemical composition of the particle, on the effective thermal conductivity of Mn-Zn ferrofluids in particular.

Specific Objectives

- Design, fabricate and calibrate a transient hot wire system to measure the thermal conductivity of different nanofluids.
- Understand the coating effect of the wire in the outcome of the hot wire system by solving numerically the heat equation for the line source case.
- Prepare and characterize water-based ferrofluids containing $Mn_xZn_{1-x}Fe_2O_4$ nanoparticles.
- Validate the accuracy and reproducibility of the measurements.

1.3 Background

1.3.1 Different techniques to measure the thermal conductivity

Generally speaking, there are a number of different techniques to measure thermal conductivity. Each of these techniques is suitable for a limited range of materials, depending on the thermal properties and the medium temperature. A distinction can be made between *steady-state* and *transient-state* techniques. In general *steady-state* techniques perform a measurement when the material that is analyzed is in complete equilibrium. This makes the process of signal analysis very easy (steady state implies constant signals). The disadvantage is that it takes usually a long time to reach the required equilibrium.

Transient-state techniques are based on the fact that one can determine the thermal conductivity of a medium from the temperature response to heating. After an initial transition period, the temperature rises close to the heater depends only on the thermal conductivity of the surrounding medium, and no longer on the heat capacity of the wire. Transient methods avoid the necessity of reaching a real thermal equilibrium by performing temperature measurement during the process of heating up. *Transient-state* techniques are fast and also there is no need for careful sample preparation. Techniques based on this principle are therefore suitable for quick experiments and it is also appropriate for field use. Some conventional methods have a temperature measurement at a large distance from the heater (typically some centimeters away, sometimes using a physically separated heater and temperature sensor). Other methods measure the temperature rise of the heater itself.

Parallel plate method:

Steady-state methods used for the measurement of the thermal conductivity of fluids and solids employs usually the geometry of parallel plate. A schematic diagram of the guarded parallel plate instrument is shown in figure 1. The sample is contained in a gap between two plates (upper and lower) maintained a distance *d* apart by spacers. A small amount of heat *Q* is generated electrically in the upper plated and is transported through the sample to the lower plate. Around the upper plate, and very close to it, is placed a guard plate. This plate is maintained automatically at the same temperature as the upper plate so as to reduce heat losses from the upper plate and to most nearly secure a one-dimensional heat flow at the edges of the sample.

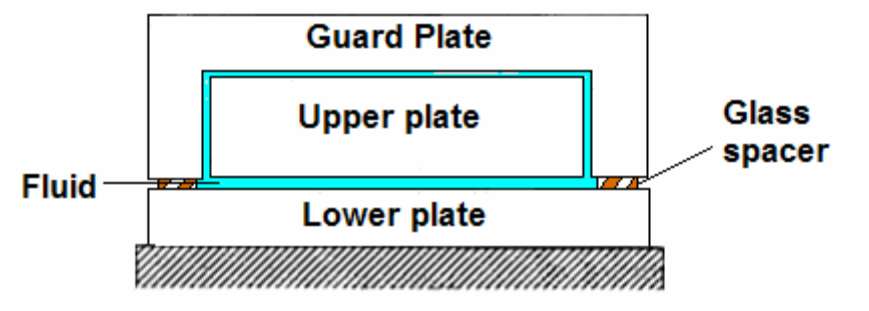

Figure 1: Representation of a parallel plate instrument

The temperatures at the surfaces of the upper and lower plates and the electric input of energy are measured very precisely, so that the thermal conductivity can be evaluated from the Fourier's law:

$$Q = \frac{Ak\Delta T}{d} \tag{1.1}$$

Where ΔT is the measured temperature difference, A is the area of the upper plate and d is the distance between the plates. From here:

$$k = \frac{Qd}{A\Delta T} \tag{1.2}$$

This technique has particular advantages in some special regions of thermodynamic space, but if accurate results are to be obtained requires great attention to details such as: radiation emissivity of the plates, the gab between the plates (have to be small as possible perhaps 0.2mm for fluids), heat transfer by convection, axial heat flow (to avoid spurious heat losses on the plates). In many cases, the effort of performing absolute measurement cannot be justified so that the ratio A/d is determined by calibration with a material of known thermal conductivity.

It is a fact of history that the necessary care with this instrument has been taken by only a few workers so that despite the fact that the instrument has been used in a wide temperature range (4K-800K) and for pressure up to 250 MPa, only some of the measurements are reliable [6].

The temperature oscillation technique

In the temperature oscillation technique a cylindrical volume is filled with a liquid specimen, forming a slab bounded above and below by a reference material. Two Peltier elements mounted on the outer surface of the reference layers generate temperature oscillations on these surfaces and temperature waves propagate through the reference into the specimen. The thermal diffusivity of the fluid is deduced by measuring and evaluating the amplitude attenuation and/or the phase shift between the fundamental temperature oscillations at the surface of the liquid specimen and at any point inside the specimen.

If the thermal diffusivity is known, the thermal conductivity is determined by the measured amplitude attenuation or the phase shift between the fundamental temperature oscillations at the surface of the reference layer and at the surface of the liquid specimen [7]. Figure 2 shows a simplified scheme of the measurement cell.

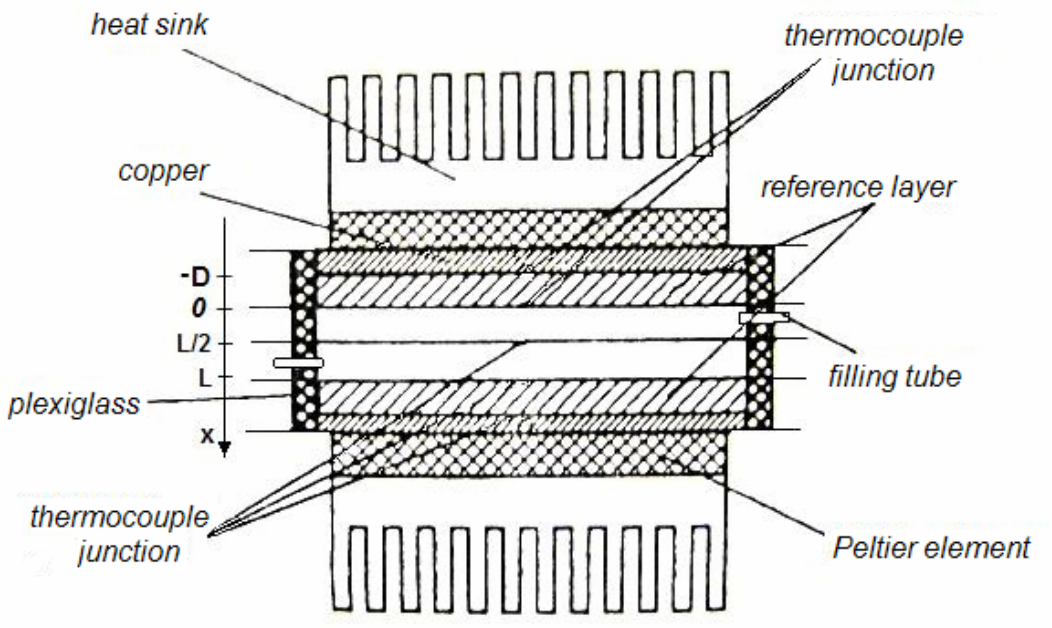

Figure 2: Schematic diagram of the temperature oscillation apparatus [7]

1.3.2 The transient hot wire method

The transient hot wire method is an experimental technique in which a constant current is passed through a thin platinum wire, embedded in a sample, and the temperature of the wire increases due to the power dissipation by joule heating after a time period. The thermal conductivity of the surrounding liquid is determined by measuring the temperature change of the wire respect to time.

The temperature variation induced by the heating of the wire, is obtained by measuring the voltage rise and then determining the resistance change. On the wire this voltage measurement must be done quickly at the very initial transient to avoid natural convection effects. The resistance values can be used to calculate the temperature variation since the resistivity of platinum shows a highly linear temperature dependence. The thermal conductivity is obtained by using the following equation [8] (see appendix for detailed analysis of the equation):

$$K = C\frac{q}{4\pi(T_2 - T_1)}Ln\left(\frac{t_2}{t_1}\right) \tag{1.3}$$

Where T_2-T_1 is the temperature rise of the platinum wire between times t_1 and t_2 and q is the applied electrical power per unit length of the wire. C is a calibration constant related to the coating and the length of the wire. The temperature is assumed uniform along the length the wire. This technique has been commonly used to measure thermal conductivities of nanofluids [9].

The transient hot-wire apparatus consists of a platinum wire suspended in a liquid in a vertical cylinder container; the coated platinum wire is used as a heater as well as a temperature sensor. For the temperature measurement, the platinum wire is used as a resistance temperature detector (RTD), making it ideal for high accuracy measurements. The platinum wire is mounted in a Wheatstone bridge to improve accuracy by reducing impedance error. The basic Wheatstone bridge contains four resistances, a voltage source and a voltage meter. A typical hot-wire system is presented schematically in figure 3.

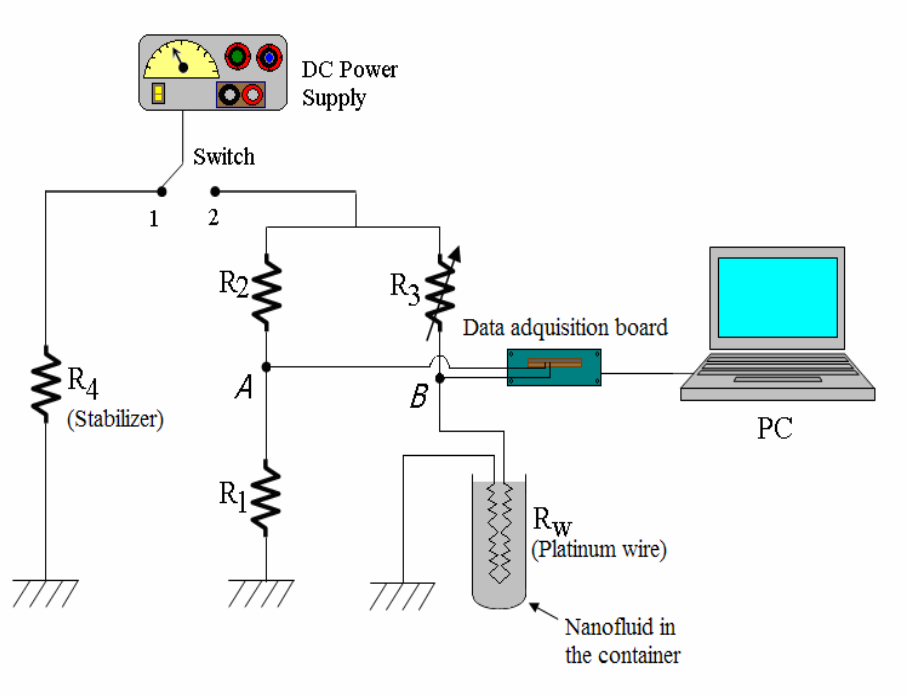

Figure 3: Schematic of a hot-wire system

The main advantages of the transient hot wire method are the almost complete elimination of natural convection effects, its fast implementation and its high accuracy [10]. The transient hotwire method was normally limited to electrically non-conducting fluids. For electrical conductive liquids, the electrical current in the wire becomes uncertain to determine. Also polarization effects take place on the wire surface, inducing uncertainties. Then, to measure thermal conductivity in electrical conducting liquids using the transient hot wire technique, the wire has to be coated with a thin electrical insulation layer [11] to prevent the current to pass through the fluid. This fact must be considered in measurements of thermal conductivity of ferrofluids since ferrofluids are likely to be electrical conductive. Then, it is necessary to calibrate a constant in order to correct the effect of the coating in the RTD.

Different techniques have been used to measure thermal conductivity of fluid. The steady-state parallel-plate technique [12], the temperature oscillation technique [7] and the transient hot wire method [10] have been employed to measure the thermal conductivity of nanofluids. Among them the transient hot wire method has been the one used more extensively in the thermal conductivity measurements of fluids.

1.3.3 Ferrofluids

This section and the next one present a more detailed description about the composition and structure of ferrofluids in order to understand the concept and the characteristics of such fluids. Also, some of the most important parameters related to effective thermal conductivity of ferrofluids are introduced since their effects will be considered.

Ferrofluids or magnetic nanofluids are stable colloidal suspensions of magnetic particles, with sizes typically of 5 to 30 nm dispersed in a liquid carrier. Volumetric concentrations of particles generally range from 1% to 10%. The ferrofluid do no simple refer to a simple liquid-solid mixture.

Some special requirements are necessary, such as homogenous/uniform suspension, suspension stability, low agglomeration of particles and chemical homogeneity of the disperse phase. A schematic of a ferrofluid composition is presented in figure 4.

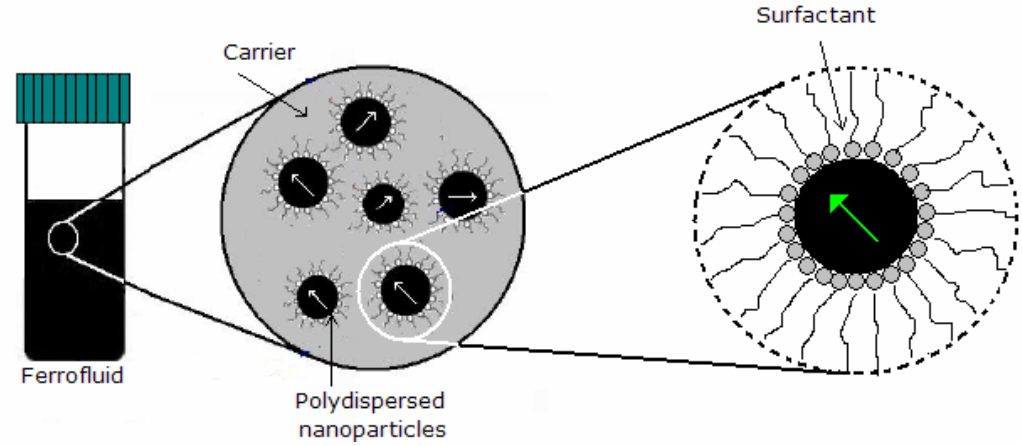

Figure 4: Ferrofluid composition schematic

In a stable magnetic nanofluid, the size of the magnetic particles must be well controlled not only to tune the magnetic behavior within the single domain limits but also to keep non-agglomerated particles in suspension even during exposure to strong magnetic fields. Particles agglomeration and subsequent settling can be avoided by using a surfactant or other type of coating [13]. The coating agent must be matched to the carrier type and it must overcome the Van der Waals and magnetic forces in order to prevent agglomeration and further precipitation of the nanoparticles.

1.3.4 Synthesis of ferrites by the co-precipitation method

The synthesis of $Mn_xZn_{1-x}Fe_2O_4$ is performed via the modified co-precipitation method following the experimental technique developed by E. Calderon, at the nanomaterial processing laboratory at UPRM [14]; among the size-reduction and microbial synthesis methods the co-precipitation method is the most popular used today [15].

In the co-precipitation method, a solution containing Fe(III) and a divalent metal cation M(II) at suitable mole ratios is mixed with a hot alkaline solution. The hydrolysis reaction leads to the formation of a mixed paramagnetic Fe-M hydroxide, which undergoes dehydration and atomic rearrangement conductive to stoichiometric ferrite structure without the need of further annealing according to:

$$2Fe^{+3} + M^{+2} + 8OH^{-} \rightarrow Fe_2M(OH)_8 \rightarrow MFe_2O_4 + 4H_2O \qquad (1.4)$$

In this work, suitable weights of Zn(II), Mn(II) and Fe(III) salts are employed to get different stoichiometric compositions. Therefore, for a certain amount of Fe(III) employed, the amount of Mn(II) and Zn(II) is fixed. The ferrite nanoparticles composition is then obtained from the atomic ratio of Mn(II) to the complete metal cation Mn(II) plus Zn(II) as follows:

$$x = \frac{Mn}{Mn + Zn} \qquad (1.5)$$

Initial molar portion of the co-precipitating agent does not maintain the stoichiometric relation and an excess of OH^{-} becomes necessary. The amount of the base and its concentration are determined experimentally [15, 16]

The nucleation rate tends to be high at the beginning of the synthesis whereas the excess of OH^{-} ions provide a net negative surface charge to the nuclei limiting their further growth and agglomeration. Under such conditions, polydisperse nanoparticles are commonly obtained [14, 16].

2. REVIEW OF LITERATURE

2.1 Experimental Investigations

Many experimental works have been reported on the measurement of the thermal conductivity of nanofluids, since this is the most important parameter responsible for enhanced heat transfer. All the experimental results have demonstrated the enhancement of the thermal conductivity by addition of nanoparticles. Alumina (Al_2O_3) and copper oxide are most common and inexpensive nanoparticles used by many researchers in their investigations.

Eastman et al. [17] reported the thermal conductivity of nanofluids containing Al_2O_3, CuO, and Cu nanoparticles with two different base fluids: water and HE- 200 oil. A 60% improvement of the effective thermal conductivity was achieved as compared to the corresponding base fluids for only 5% of volumetric concentration of nanoparticles.

Lee et al. [18] suspended CuO (18.6 and 23.6 nm) and Al_2O_3 (24.4 and 38.4 nm) using two different base fluids: water and ethylene glycol (EG) and obtained four combinations of nanofluids. Their results showed that nanofluids have significantly higher thermal conductivities than the base fluid more than 20% at 4% of volumetric concentration of CuO nanoparticles with EG as base fluid. In the low volume concentration range the effective thermal conductivity increase almost linearly with volumetric concentration.

Eastman et al. [19] used pure Cu nanoparticles of less than 10 nm size and achieved 40% increase in thermal conductivity for only 0.3% of volumetric concentration with ethylene glycol as base fluid.

They indicated that the increased ratio of surface to volume with decreasing size should be an important factor. Also, they showed that the additive acid may stabilize the suspension and thus increase the effective thermal conductivity.

Murshed et al. [20] investigated TiO_2 nanoparticles in rod-shape (d=10nm and l=40nm) and spherical shape (d=15 nm) dispersed in deionized water. They observed that nearly 33% and 30% enhancement of the effective thermal conductivity occurred for TiO_2 particles of rod-shape and spherical particles, respectively. Results showed that both particle size and shape influence the thermal conductivity of nanofluids.

A Fe-nanofluid was prepared by Hong and Yang [21] with ethylene glycol; Fe nanoparticles with mean size of 10 nm were produced and they found that Fe nanofluids exhibited higher enhancement of thermal conductivity than Cu nanofluids. Their result indicated that the material with high thermal conductivity is not always the best candidate for the suspension to improve the thermal characteristics of base fluids.

The disagreement among the different groups should rely on the differences associate with: the properties of the particles used, the shape and the size of the nanoparticles, the inclusion of dispersants, the base fluid used and the experimental errors involved in each one of the investigations. It is inappropriate to compare results from different investigations just based in the fact that they were using the same kind of particles and the same volumetric concentration of nanoparticles because the other mentioned parameters also affect the thermal conductivity of nanofluids.

2.2 Thermal conductivity models

There are no theoretical formulas currently available to predict satisfactorily the observed thermal conductivity enhancement of nanofluids. However, there exist several semi-empirical correlations to calculate the apparent conductivity of two-phase mixtures.

Classical models

The classical models are derived from continuum formulations and include only thermal conductivities of the base fluid and thermal conductivity of the nanoparticles, particle shape and volume fraction and assumed diffusive heat transport in both liquid and solid phases. They are mainly based on the following definition of the effective thermal conductivity of a two-component mixture:

$$k_{eff} = \frac{k_p \phi_p (dT / dx)_p + k_f \phi_f (dT / dx)_f}{\phi_p (dT / dx)_p + \phi_f (dT / dx)_f} \tag{2.4}$$

The first theoretical study conducted for particle-fluid mixtures was the classical work of Maxwell. The Maxwell-Garnett model (MG model) correlates the effective thermal conductivity of nano fluids K_{eff} with the thermal conductivity of solid spherical particles k_p, the base fluid k_f and the volume concentration of the particles ϕ [1]. It is given by:

$$K_{eff} = \frac{k_p + 2k_f + 2(k_p - k_f)\phi}{k_p + 2k_f - (k_p - k_f)\phi} k_f \tag{2.5}$$

The MG model has been successfully applied for explaining the thermal conductivity of solid-solid composites and to solid–liquid mixtures of relatively large particles (micro-/mini-size). It is good for low volumetric concentration of solid particles.

What is even more confusing is that for nanosized particles, the impact of any interfacial resistance should be pronounced, and would tend to decrease the enhancement in the thermal conductivity of the composite system as compared to micron-sized particles [22]. Recently Wilson et al. [23] and Huxtable et al. [24] experimentally measured the interfacial thermal resistance (R_b) between nanoparticles and different fluids.

The magnitude of R_b in their study ranged from low ($\approx 0.77\times10^{-8}$ Km^2W^{-1}) to high values ($\approx 20\times10^{-8}$ Km^2W^{-1}). The MG model for thermal conductivity of a composite with interfacial thermal resistance and for highly conductive particles as compare to the fluid ($k_p >> k_f$), is given by [22]:

$$\frac{k_{eff}}{k_m} = \frac{(1 + 2\alpha) + 2\phi(1 - \alpha)}{(1 + 2\alpha) - \phi(1 - \alpha)} \tag{2.6}$$

Where $\alpha = 2R_b\ k_f /d$ is the nanoparticle Biot number and d is the particle diameter. Equation (2.6) shows that for $\alpha > 1$, K_{eff} is lower than k_f and will continue to decrease with increasing ϕ.

Figure 5 presents a plot of equation (2.6) for different values of R_b and shows that K_{eff} can be smaller than k_f, depending on the value of R_b, even for the case where $k_p >> k_f$. A critical diameter of the particle can be defined, below which $K_{eff} < k_f$. The critical diameter d_c is given by $\alpha = 1$, i.e., $d_c = 2R_b k_f$ such that $K_{eff} = k_f$. Also Figure 5 shows that even for R_b as low as 1.925×10^{-8} Km^2W^{-1}, d_c is approximately 10 nm for ethylene glycol based nanofluids with a volumetric concentration $\phi = 0.05$.

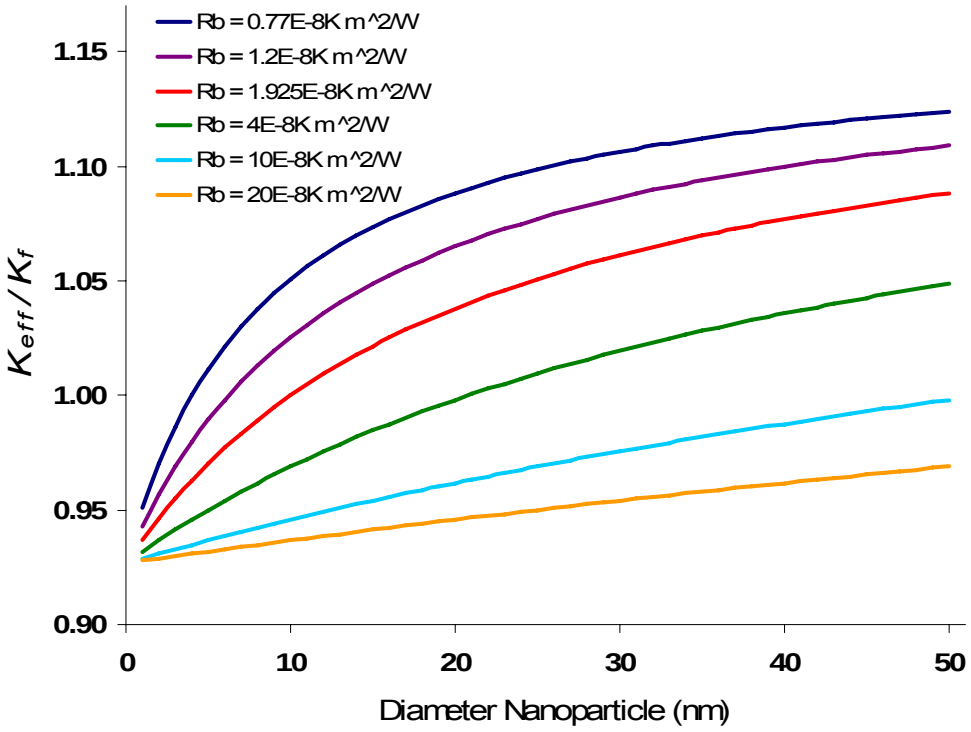

Figure 5: Effect of particle diameter and interfacial thermal resistance Rb on the effective thermal conductivity predicted by the Maxwell-Garnett model

Nan et al. [22] have experimentally shown that $K_{eff} < k_f$ in composites made from zinc sulphide filled with diamond particles, and silicon carbide filled with aluminum due to the presence of R_b. Below d_c these nanoparticles, in spite of having high thermal conductivity, reduce K_{eff} because of the interface resistance.

Bruggeman [25] proposed a model to analyze the interactions among randomly distributed particles. For a binary mixture of homogeneous spherical inclusions, Bruggeman model gives:

$$\left(\frac{k_p - k_{eff}}{k_p + 2k_{eff}}\right) + (1 - \phi)\left(\frac{k_f - k_{eff}}{k_f + 2k_{eff}}\right) = 0 \qquad (2.7)$$

The solution of the above quadratic equation is given as:

$$k_{eff} = (3\phi - 1)k_p + [3(1 - \phi) - 1]k_f + \sqrt{\Delta} \quad (2.8)$$

Where:

$$\Delta = (3\phi - 1)^2 k_p{}^2 + [3(1 - \phi) - 1]^2 k_f{}^2 + 2[2 + 9\phi(1 - \phi)]k_p k_f \quad (2.9)$$

Bruggeman model has no limitation on the concentration of inclusions, and can be used for spherical particle percolation in suspensions. For low particle-concentration suspension, the Bruggeman model shows almost the same result as the MG model will give. For a particle percolation situation or when the particle concentration is sufficiently high, the MG model fails to predict precisely the experimental results, while the Bruggeman model can still fit well with experimental data.

Hamilton and Crosser [26] proposed a model for liquid–solid mixtures for non-spherical particles, by introducing a shape factor, n, to account for the effect of the form of the particles. The thermal conductivity, in which the ratio of conductivity of the solid and fluid phases is larger, than 100 ($k_p/k_f > 100$), can be expressed as follows:

$$k_{eff} = \frac{k_p + (n - 1)k_f - (n - 1)(k_f - k_p)\phi}{k_p + (n - 1)k_f + (k_f - k_p)\phi} k_f \quad (2.10)$$

Where n is the empirical shape factor given by $n = 3/\psi$, and ψ is the particle sphericity, defined as the ratio of the surface area of a sphere with volume equal to that of the particle, to the surface area of the particle. Comparison between equations (2.10) and (2.5) reveals that Maxwell's model is a special case of the Hamilton and Crosser's model for sphericity equal to one.

Recently models

Some important mechanisms in nanofluids appear to be neglected in the classical models presented above. Many researchers investigated possible factors of enhancing thermal conductivity in nanofluids such as the clustering, concentration and size of particles, Based on the traditional models, many later theoretical works have been proposed to address such effects, especially the interfacial characteristics and the Brownian effect.

In 2003 Xuan et al. [27] proposed a modified formula for the effective thermal conductivity based on the Maxwell model and considering the Brownian motion of suspended nanoparticles. Koo and Kleinstreuer [28] developed a new model for nanofluids, which includes the effects of particle size, particle volume fraction as well as properties of the base fluid and the particle subject to Brownian motion.

In 2005 Xue and Xu [29] obtained an equation for the effective thermal conductivity according to Bruggeman model [25]. Their model takes account of the effect of interfacial shells by replacing the thermal conductivity of nanoparticles with the assumed thermal conductivity of the so-called "complex nanoparticles", which included the interfacial shells between the nanoparticles and the base fluids. On the other side, Prasher [32] proposed that convection caused by Brownian motion of the nanoparticles is primarily responsible for the enhancement in the effective thermal conductivity of nanofluids. By introducing the general correlation for heat transfer coefficient h, Prasher modified the Maxwell model by including the convection of the liquid near the particles due to Brownian movement.

2.3 Mechanism for thermal transport in nanoscale

As mentioned before, nanofluids exhibit superior heat transfer characteristics to conventional heat transfer fluids and the parameter used to measure the increase in the thermal conductivity of the base fluid caused by the nanoparticles is the quotient between the effective thermal conductivity of the ferrofluid K_{eff} and the thermal conductivity of the base fluid K_f. The reasons to explain that enhancement are not such clear, even when numerous studies have been conducted intending to explain the factors and the mechanisms that affect the thermal conductivity of particle-fluid mixtures. Based on the large enhancement of the effective thermal conductivity of nanofluids observed in experimental results can be concluded that the macroscopic theory of heat transport in composite materials fails for the case of nanofluids. In this section a comprehensive list of the factors that are potentially responsible for the inadequacy of the theory are examined. This analysis will narrow the list of mechanism capable of explaining the unusual enhancement of heat transport in nanofluids.

Brownian motion

In 1827, Scottish botanist named Robert Brown found the "Brownian Motion". He observed the pollen suspended in the water had irregular motions under a microscope. Today it is known that Brownian motion of particles in a liquid is due to the instantaneous imbalance in the force exerted by the small liquid molecules on the particle. This motion can be expected to increase thermal conductivity by enabling direct solid-solid transport of heat from one to another particle, when particles move through the liquid and possibly collide.

This is not accounted for by the classical theories which assume a static composite material. Brownian motion is characterized by the particle diffusion constant D given by the Stoke-Einstein formula [30]:

$$D = \frac{k_B T}{3\pi\eta d} \tag{2.1}$$

Where k_B is the Boltzmann constant, η is the fluid viscosity and d is the particle diameter. Time required by Brownian diffusion, "τ_b", is the time required by a particle to move a distance equal to its size and it is given by:

$$\tau_b = \frac{3\pi\eta d^3}{6k_B T} \tag{2.2}$$

Keblinski et al. [30], calculated the time required by Brownian diffusion versus the time required for the heat diffusion on the liquid and they showed that energy transport due to the Brownian diffusion is two orders of magnitude smaller than energy transport due to conduction in the liquid. However, Brownian motion could have important indirect role in producing particle clustering or in the energy transport due to convection caused for the movement of the particle. This, as it will be described later, could significantly enhance thermal conductivity.

Liquid layering at liquid/particle interface

Contrary to the effect of the interfacial resistance in thermal conductivity, that arise from the formation of a week interfacial contact, an interface effect that could enhance thermal conductivity is the observed layering of the liquid at the solid interface [31], by which the atomic structure of the liquid layer is significantly more ordered than that of the liquid solid. This layering at the interface is expected to lead to a higher thermal conductivity,

since crystalline solids, which are evidently ordered, display much better thermal transport than liquids. Keblinski et al. [30] estimated an upper limit for this effect by assuming that the thermal conductivity of the interfacial liquid is the same as that of the solid and showed that the resultant large effective volume of the particle-layered-liquid structure would enhance the thermal conductivity. Figure 6 shows the effective thermal conductivity enhancement for four different layer thickness "*h*" as a function of the particle diameter and assuming the same thermal conductivity for the layer and for the solid particle. The larger the thickness of the layer around the particle, the higher the effective thermal conductivity.

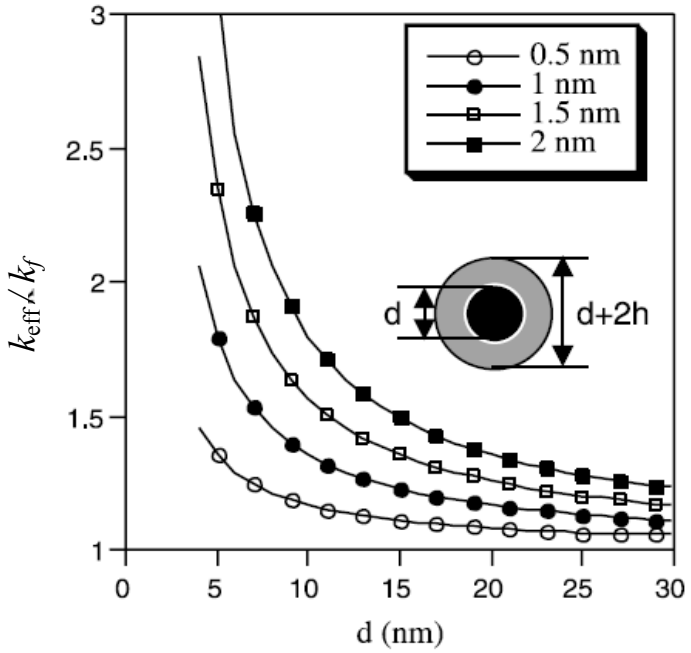

Figure 6: Effective thermal conductivity due to formation of highly conductive layered-liquid structure at liquid/particle interface [30]

Although the presence of an interfacial layer may play a role in heat transport, it is not likely to be solely responsible for the enhancement of thermal conductivity, especially when the observed increase is more than an order of magnitude larger than that predicted by the classical theoretical models.

Nature of heat transport in nanoparticles

In crystalline solids, such as those used in nanofluids, heat is carried by phonons, i.e., by propagating lattice vibrations. Such phonons are created at random, propagated in random directions, are scattered by each others or by defects, and thus justify the macroscopic description of heat transport. Based on the determination of the mean free path of a phonon, Keblinski et all. [30] show that phonons cannot diffuse in a small particle because the mean free path of the phonon is bigger than the particle diameter. They suggest that the phonons must move ballistically across the particle.

Even though macroscopic theory assumes diffusive heat transport, this analysis demonstrates that the assumption of diffusive heat transport in nanoparticles is invalid. Consequently the classical thermal conductivity models, based on the macroscopic theories, do not apply and a theoretical treatment based on ballistic phonon transport is required. However it is difficult to envision how ballistic phonon transport could explain the larger increase of thermal conductivity in nanofluids, from the macroscopic point of view.

On the other hand, other ballistic phonon effects could lead to a significant increase in thermal conductivity, in particular, if the ballistic phonons from one particle cross the liquid boundary and reach adjacent particles. This effect only may operate if the separation between particles is small, likely on the order of the thickness of the layered liquid (≈1-2 nm).

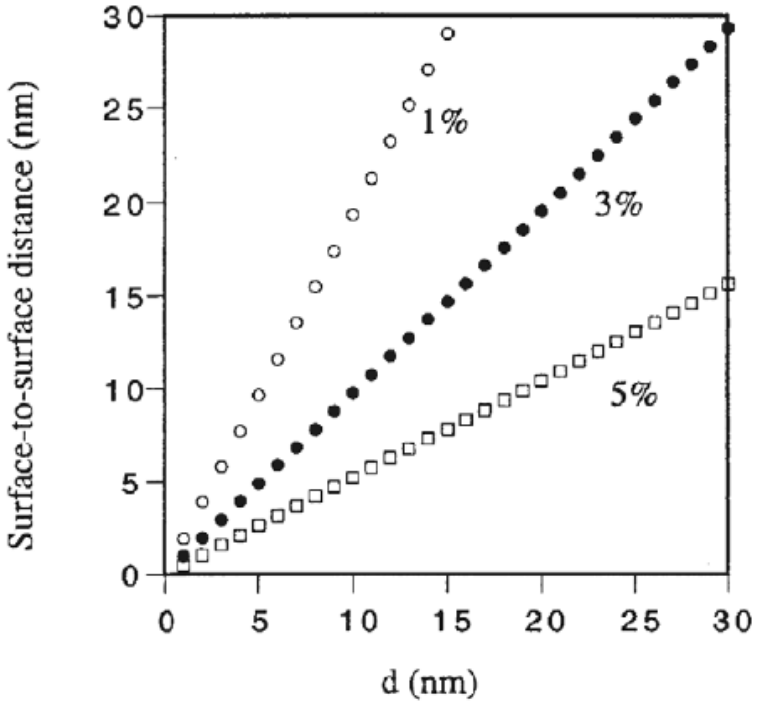

Figure 7: Average distance between particles due to the particle diameter d [30]

Figure 7 shows the relationship between the average surface-to-surface particle distance and the particle diameter, both axis in nanometers, for three different volumetric concentrations. According to this figure the bigger the diameter, the larger the average distance between the surfaces of the particles and by increasing the volumetric concentration, the particles get closer.

As illustrated in figure 7, the particles in a nanofluid are surprisingly close together even at relatively low packing fractions. Furthermore, the particles may be much closer locally, due to the constantly movement caused by the Brownian motion, enhancing in this way the coherent phonon heat flow among the particles.

Effects of nanoparticle clustering

Clustering of particles into percolating pattern would have a major effect on the effective thermal conductivity by creating path of lower thermal resistance. But clustering to span large distances is unlikely, due to the lack of stability. Although the percolation lower limit for random dispersion in three dimensions is ≈15% volumetric concentration, the unusual enhancement of thermal conductivity is already observed at very low volumetric concentration ≈1% and less [4]. Even though percolating structures can no be established, local clustering is possible and indeed has been observed experimentally [19].

The effective volume of a cluster, i.e. the volume from which other clusters are excluded, can be much larger than the physical volume of the particles. The effective volumetric concentration of the particles, inside a cluster, is larger than the volume of the solid phase, since within such cluster heat can move very rapidly. According to classical models, further explained, this effect may significantly increase the thermal conductivity.

The effective volume of a cluster "Φ" is defined as the ratio of the volume of the solid particles in the cluster to the total volume of the cluster. Figure 8 shows the effective thermal conductivity enhancement, due to the increased effective volume of highly conducting clusters "Φ". The thermal conductivity grows with decreasing packing fraction, by increasing the effective volume of a cluster. This figure indicate: i- closely packed arrangement of particles, ii- simple cubic arrangement, iii- loosely packed irregular structure of particles in physical contact, and iv- clusters of particle separated by liquid layers thin enough to allow rapid heat flow among particles.

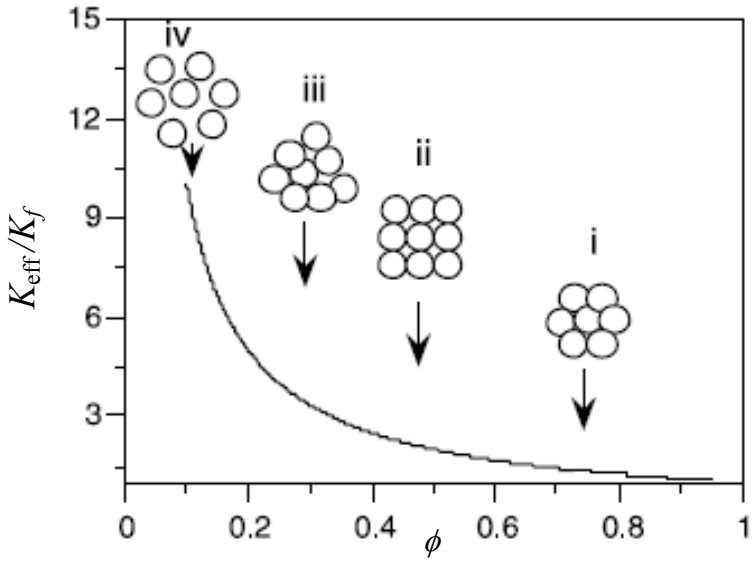

Figure 8: Thermal conductivity enhancement K_{eff}/K_f due to increased effective volume of highly conducting cluster [30]

A further dramatic increase of K_{eff}/K_f can be observed in the last case, due to the ballistic phonon transport explained before. Such "liquid-mediated" cluster exhibit a very low packing fraction and thus a very large effective volume and, in principle, are capable to explaining the large experimentally enhancements of thermal conductivity.

Convection due to the Brownian motion of nanoparticles

Similar to the analysis done to study the effect of the Brownian motion, Prasher et al. [32] performed an analysis regarding the time scale of the convection due to the movement of the particle and the energy transport caused for it. They showed trough an order of magnitude analysis that the enhancement in the effective thermal conductivity of nanofluids is due mainly to the localized convection caused by the Brownian movement of the nanoparticles. The convection diffusivity is the kinematic diffusivity of the liquid, i.e., the momentum diffusivity. Therefore the time required for the effect of convection "τ_c" to be felt at a distance equal to the nanoparticle diameter d, is given as:

$$\tau_c = \frac{d^2}{\nu} \tag{2.3}$$

Where ν is the kinematic viscosity of the liquid and is defined by $\nu = \eta/\rho$. Prasher et al. [32], using equation (2.3), calculated the time required by the propagation of the convection effect versus the time required by Brownian diffusion "τ_b" and they showed that the time required by the propagation of the convection is three order of magnitude smaller than time required by Brownian diffusion in water and five order of magnitude smaller in ethylene glycol. This simple analysis shows that $\tau_c << \tau_b$ or that the effects of convection are propagated almost instantaneously relative to the Brownian diffusion of the particle. They show that the lighter the nanoparticles, the greater the convection effect in the liquid, regardless of the thermal conductivity of the nanoparticles.

Surface chemical effect

One of the current technological limitations is the suspension stability in the nanofluids. As the colloidal system becomes less stable, particles are aggregated, leading to changes in the hydrodynamic size as well as morphology and sometimes in volume fraction by settling down. A coating agent is used to prevent agglomeration and further precipitation of the nanoparticles. Note that the surface chemical treatment changes the suspension stability through surface charge states and resultant surface potential.

Lee et al. [33] found that higher surface charges facilitate heat transport more effectively by changing pH of the CuO-water nanofluid systematically to control surface charge density and surface potential (that can be reflected by ζ potential) and measuring the thermal conductivity .

Figure 9 shows the effective thermal conductivity enhancement due to the changes in Ph of CuO-water nanofluid for ϕ=0.3%. This figure shows that the effective thermal conductivity (K_{eff}) increases by a factor of 3 as pH decreases from 8 to 3. The enhancement seems to be related only to particles, because the thermal conductivity of base fluid is nearly constant at different doses of electrolyte salt and acid or base. Also they found that the surface charging effect is indeed true over the whole range of volume fraction.

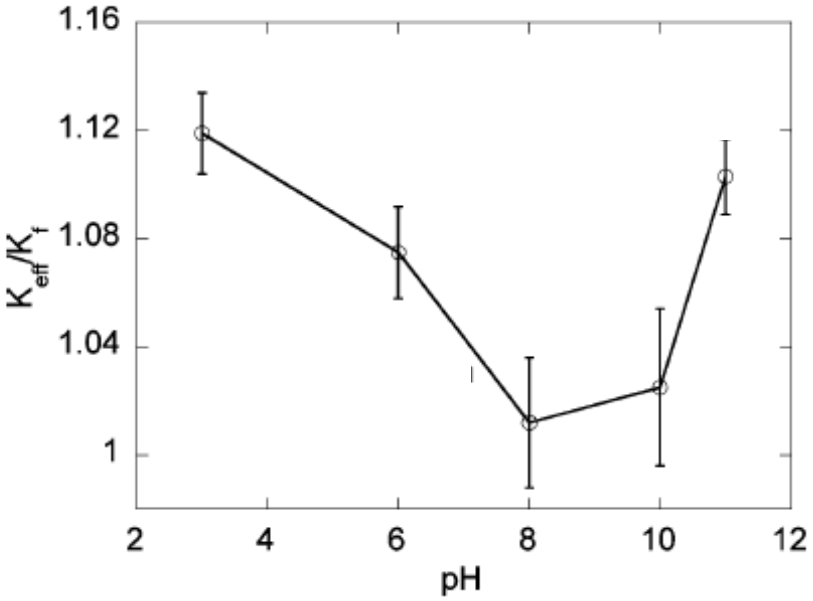

Figure 9: Effect of pH on the thermal conductivity of the CuO-water nanofluid [34]

The charges seemingly transport heat more efficiently and it can be inferred that the charged surface sites provide much more effective passages through which heats or phonons are going. Xue et al. [34] showed from molecular dynamic simulation that phonons felt much less resistance during travel from particle to liquid at stronger interfacial bonding. Therefore, it looks reasonable to infer that lower pH or higher surface charging condition facilitates phonon transport through increases of effective sites and transport efficiency.

The ionized surface groups attract counterions and they attracts others indifferent ions from the outer region, forming in this way cylindrical ordered structures. Such ordered liquid structure, at the particle surface, is likely to act as a part of the solid, leading to the effective increase of the volume fraction. The previous concept of the interfacial layer may be related to this one.

Others mechanisms

Although the mechanisms explained above are the most important there are others mechanisms that also contribute to the thermal conductivity of the nanofluids; among them, the increased ratio of the surface area to volume for a particle and the thermophoresis.

The suspended nanoparticles increase the solid surface area of the fluid. For instance the ratio of the surface area to volume for a particle with 20 nm diameter is 5 times larger than that for a particle with 100 nm diameter, a dramatic improvement in effective thermal conductivity of nanofluids is expected by decreasing the particle size.

Thermophoresis refers to the motion of colloidal particles in response to a temperature gradient. The thermophoretic effect can be explained by applying the kinetic theory. The high energy molecules in the hot region of the liquid impinge on the particles with greater momentum than do molecules coming from the cold region, thus leading to the migration of the particles in the direction opposite to the temperature gradient. This mechanism has been found to be negligible, primarily because of the very small particle migration velocity [28].

2.4 Contribution of this research

This research contributes to a better understanding of the influence of different parameters on the effective thermal conductivity of nanofluids and in particular Mn-Zn ferrofluids.

A systematic analysis is implemented in order to characterize the ferrofluids and get detailed information of the ferrofluids. The thermal conductivity of such fluids will be evaluated varying the nanoparticle diameter, the base fluids, the volumetric concentration and chemical composition of the nanoparticles. The transient hot wire method is implemented to measure the effect of each one of those parameters and compared with the results obtained for similar fluids, since there is not previous thermal characterization of this kind of fluid. Controversial aspects of the transient hot wire method and its effectiveness for this kind of measurements are discussed, especially the coating effect of the wire in the outcome of the hot wire system and its importance in the measurement of electrical conducting fluids such as the ferrofluids. The synthesis of nanoparticles and ferrofluid was performed based on the work done by Perales et al. [16]. In addition, the different nanoparticles are characterized via X-ray diffraction.

3. METHODOLOGY

3.1 Transient hot wire system design and calibration

The hot-wire apparatus consists of a platinum wire suspended in a liquid in a vertical cylinder container; the platinum wire is used as a heater as well as a temperature sensor. For the temperature measurement, the platinum wire is used as a resistance temperature detector (RTD), making it ideal for high accuracy measurements. The platinum wire is mounted in a Wheatstone bridge to improve accuracy by reducing impedance error. The basic Wheatstone bridge contains four resistances, a voltage source and a voltage meter. The values of the resistances and the description of the elements used in the experimental setup are presented in the table 1.

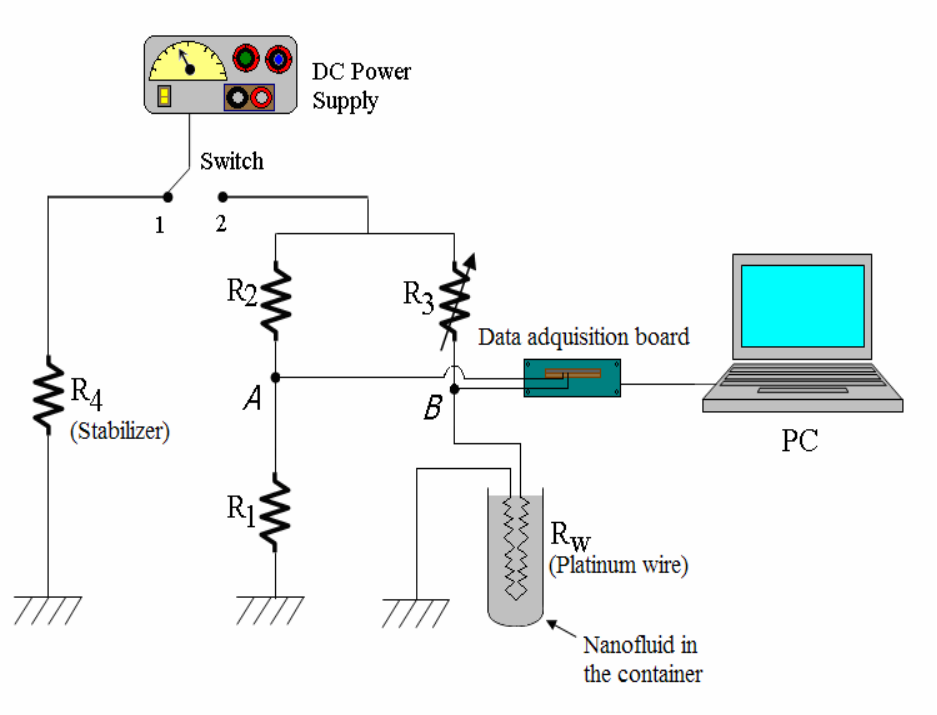

Figure 10: Representation of a transient hot-wire system

Table 1: Material list of the hot wire system

Item	Qty	Description
DC Power Supply	1	DC Power Supply GP-4303TP(0 - 20 VDC)
Data Acquisition Board	1	National Instrument SCB-68
Ammeter	1	Hewlett Packard 34401A Multimeter (0-1A)
Platinum Wire	1	Omega 100Ω-0°C, 50μm diameter and 63mm length
Power Switch	1	8121-C&K U.S.A
Resistance: R1 and R2	2	500Ω
Resistance: R3	1	Variable resistance 1KΩ
Stabilizer: R4	1	180Ω
Operational Amplifier	1	LM741 Vcc: 15v, Vin: 30mv-150mv, Po=65-100mW
Cylinder Glass	1	Numbered 20ml, 25mm diameter.

The balancing of the circuit must be done with the vertical cylinder container empty. The circuit is said to be balanced when the reading from the voltage meter (V_{AB}) is zero [35] and the relation between the resistances is:

$$\frac{R_1}{R_2} = \frac{R_W}{R_3} \tag{3.1}$$

R_1 is a variable resistance and is set to balance the circuit initially.

The first step in the procedure to acquire data is to balance the Wheatstone bridge while the switch in position 2 (follow all the measurement process from the schematic figure10) is energizing the bridge. Then, as current flows through the platinum wire embedded in a sample its resistance changes and the system becomes unbalanced. The equation for the unbalanced circuit is:

$$\frac{V_{\_AB}}{V_{\_Supply}} = \frac{R_1}{R_1 + R_2} - \frac{R_W}{R_W + R_3} \tag{3.2}$$

The next step is to start recording data with the data acquisition system. Voltage reading between points "A" and "B" of the bridge are recorded during six seconds, at 0.05 seconds intervals. The cycle begins with the switch in position 1 and during the first seconds the switch is changed to position 2. The data obtained during the first second is neglected, because of the unstable behavior of the current "I" in the bridge, when it is increasing from 0 to the maximum current (see figure 11).

R_4 is used as stabilizer in order to decrease the initial time of the current in the bridge, since R_4 is the equivalent resistance of the bridge. Hence the current from the power supply when the switch is in both positions, 1 and 2, is the same. This current produces a significant increase on the temperature of the wire and, as can be seen from equation (1.15), the temperature change of the wire depends on the thermal conductivity of the surrounding liquid.

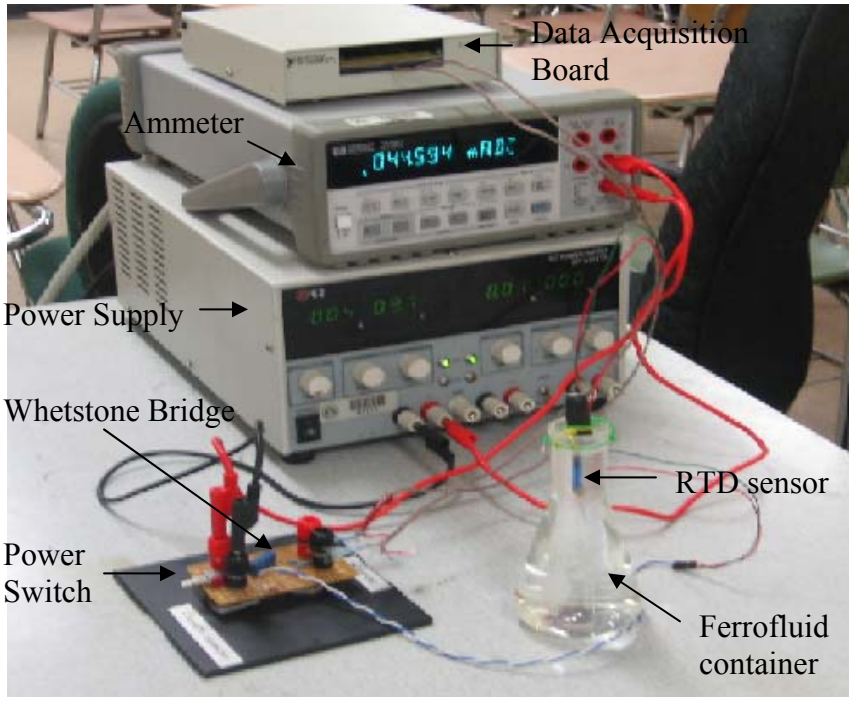

Figure 11: Experimental transient hot-wire system

The equation that correlates the resistance of the platinum wire with its temperature is obtained from a calibration curve by placing the platinum wire at three different known temperatures and measuring its resistance. The temperatures used for the calibration were 0°C (freezing point of water), 22°C (ambient temperature) and 100°C (boiling point of water). The relationship observed between temperature and resistance was very linear, even for a small change in the value of the temperature. The linear relation obtained for the temperature operation range was:

$$T = 265R_W - 267.03 \tag{3.3}$$

Note: this regression line was obtained for a temperature range of 0°C to 100°C

The measured voltage from the hot-wire apparatus is used to determine the resistance R_W of the coated platinum wire from equation (3.2), and then this resistance value is used to calculate the temperature from equation (3.3). Then, temperature vs. time is curved fitted using a logarithmic scale for the time axis to linearize the acquired data, since the temperature and the logarithm of time has a lineal relationship according to equation (1.15). The departure of the data from the straight line at early times is due to the unstable behavior of the current "I" in the bridge, while it is increasing from 0 to the maximum current. Finally the thermal conductivity is obtained from equation (1.17) using the value of the slope of the fitted curve, the value of the constant "C" and the applied electric power "q".

q is assumed to be constant, because the uncertainties associated with the change of the resistance of the wire (≈0.6Ω) due to the increases of the temperature (≈4°C) from the

initial to the maximum temperature, are around 0.42%, since the change in the current value is approximately 0.20 mA.

The constant C is a calibration constant used to correct the coating effect of the wire and has to be determined from measurements of the thermal conductivity of known fluids. For this purpose Acetone, Water and N-heptane were used. Each time the coating of the wire is changed this constant has to be recalibrated and obtain a new value of C. Common values for C can vary between 1 and 1.2. Measurements to corroborate the accuracy of the device are presented in table 2.

It is important to remark that for corrosive fluids which is typically the case of ferrofluids due to the presence of the acid surfactants used for stabilization of the nanoparticles, the coating is degradated with time and the sensor has to be recoated and calibrated again.

Table 2: Deviations of the measured thermal conductivities from their reference values

Fluid	Reference value	Measured value	Deviation
Acetone	0.1800 W/m K	0.1849 W/m K	0.088 %
N-Heptane	0.1300 W/m K	0.1249 W/m K	0.726 %
Water	0.6000 W/m K	0.5956 W/m K	0.60 %

After the sensor has been calibrated it can be used to determine the thermal conductivity of the fluid of interest. Figure 12 shows the lineal relationship between Temperature vs. Ln(time) for the experimental measurement of the thermal conductivity of one of our ferrofluid.

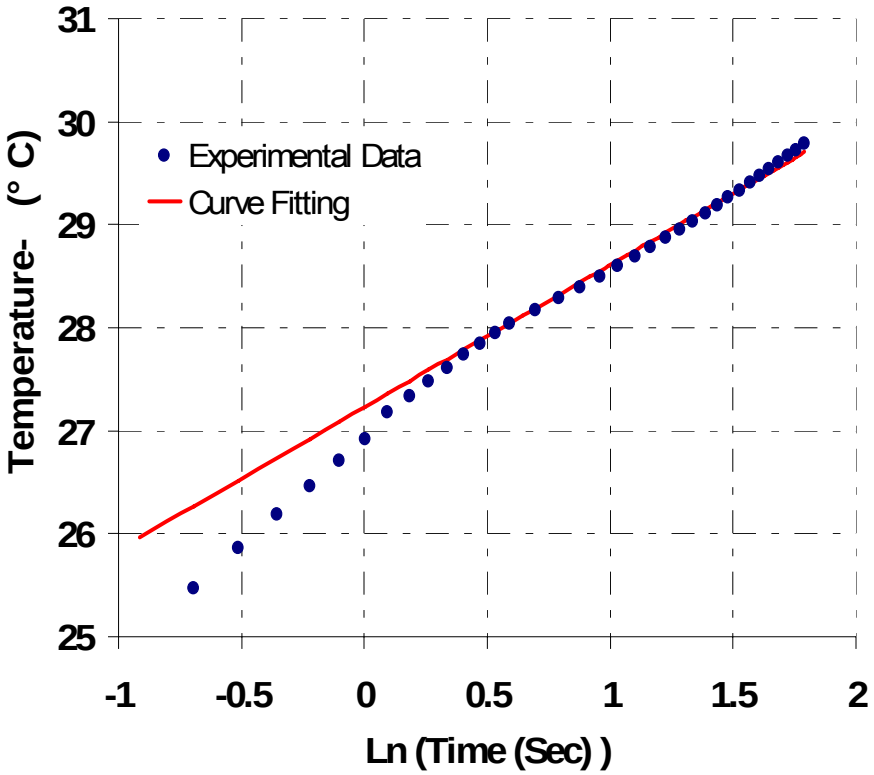

Figure 12: Temperature vs. Ln (Time(Sec)) for $Mn_{0.7}Zn_{0.3}$ ferrofluid with a 1.52% volumetric concentration

It can be seen from figure 12 the departure of date from the straight line due to the stabilization of the current in the bridge. After Ln(time) = 0.2 (1.22 seconds) the data fit with a very good agreement with a straight line. Calculating the slope $(T_2-T_1)/Ln(t_2/t_1)$, the thermal conductivity is determined from equation (1.17) by reading the current and the voltage in the bridge ($q=V\times I$) and using the calibration constant previously obtained.

In the experiments, the effect of the coating is taking account by the calibration constant. Since the thickness of the coating will change due to degradation and delusion of the coating material, the calibration constant have to be recalculated before each set of measurements to avoid the usage of a wrong constant.

3.2 Nanoparticles synthesis and ferrofluid preparation

Nanoparticle synthesis

Prior the ferrofluid preparation, synthesis of suitable $Mn_xZn_{1-x}Fe_2O_4$ nanoparticles was conduced by adding the metallic salts mixture to the pre-heated co-precipitant solution according to Calderon and Perales method. The metallic salts employed were Iron (III) chloride Hexahydrate ($FeCl_3.6H_2O$), Manganese (II) chloride Tetrahydrate ($MnCl_2.4H_2O$) and Zinc chloride ($MnCl_2$) and the co-precipitant agent used was sodium hydroxide (NaOH) at 0.5 mol/L. Keeping constant fluid volume and temperature conditions the reaction time for the ferrite nanoparticles formation was approximately 1 hour under a strong agitation rate. A schematic of the synthesis procedure is shown in figure 13.

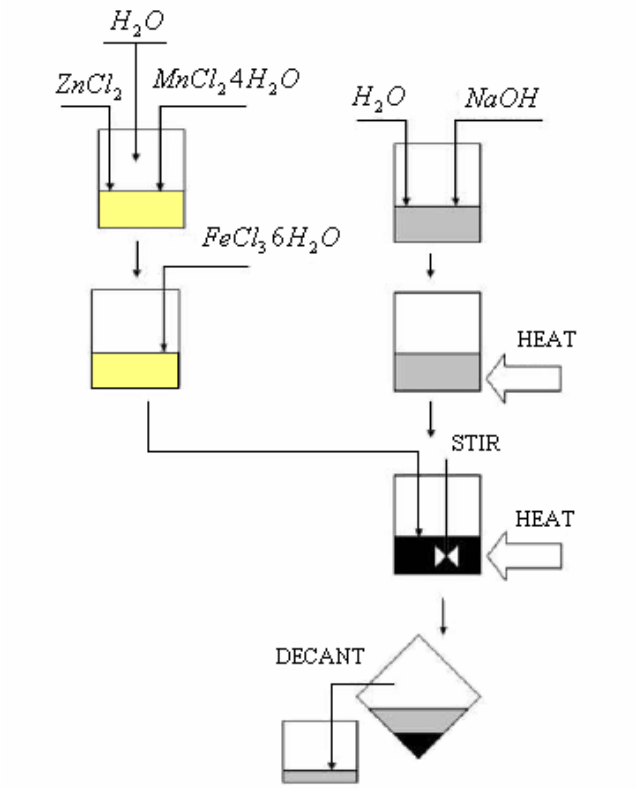

Figure 13: Synthesis Procedure Diagram [15]

The following is a detailed systematic procedure for the ferrite synthesis process. A 2000mml beaker is filled with 800ml of distilled water and the 15.64g of NaOH are added inside it. Another 2000ml beaker is filled with the $FeCl_3.6H_2O$, $MnCl_2.4H_2O$ and $ZnCl_2$ composites within 424ml distilled water while the NaOH solution is being preheated by using the burner under an agitation rate of 150rpm.

The thermometer is clamped to the beaker and the stirrer paddle is used as a level indicator. Once the NaOH solution reaches 100ºC, the salts solution is slowly added. The agitation rate is increased to approximately 900rpm and the reaction time begins when the solution reaches the boiling point. The volume of the solution must be maintained constant by adding small amounts of distilled water periodically. The reaction time was kept constant at one hour. After that the powder was magnetically recovered and washed with water several times. Part of this powder is dried at 80°C for the material characterization.

Ferrofluid preparation

For ferrofluid preparation, the nanoparticles are removed from the water used for the synthesis process and deposited in the 50ml Benchtop Centrifuge recipients. Now the recipients containing the nanoparticles are filled with the HNO_3 solution and cleaned by 15 minutes in an ultrasonic bath. Then, the washed ferrites are centrifuged as described before. The process is repeated three consecutive times until the ferrites have been completely cleaned and positively charged. Thus, Tetramethylammonium hydroxide is slowly added by using the 25ml precision probe. The resultant colloid is the ferrofluid and the sediment is discarded.

Usually the nanoparticles suspension process takes approximately two hours, the total time needed to produce the ferrofluid is three hours and the amount of ferrofluid obtained from the process is 32ml.

The obtained nanoparticles were washed with a 2mol/L nitric acid (HNO3) solution and centrifuged after manual agitation at 3600rpm for a seven minutes period, where the nitric acid cleans and provides the nanoparticles surface with a positive electrostatic charge (first layer). Then a negative surface electrostatic charge (second layer) is provided to the cleaned particles by slowly adding a 25 % water solution of tetramethylammonium hydroxide. This step completes the double-layer surfactant coating of the particles by inhibiting their agglomeration and further sedimentation. The mixture of the water, surfactant and nanoparticles is again strongly agitated prior a twelve minutes centrifugation process at 3600rpm. Figure 14 shows the double layer surfactant coating of the ferrite nanoparticle, where the small red atoms (nitric acid) are the positive layer and the blue molecules (tetramethylammonium hydroxide) are the negative layer.

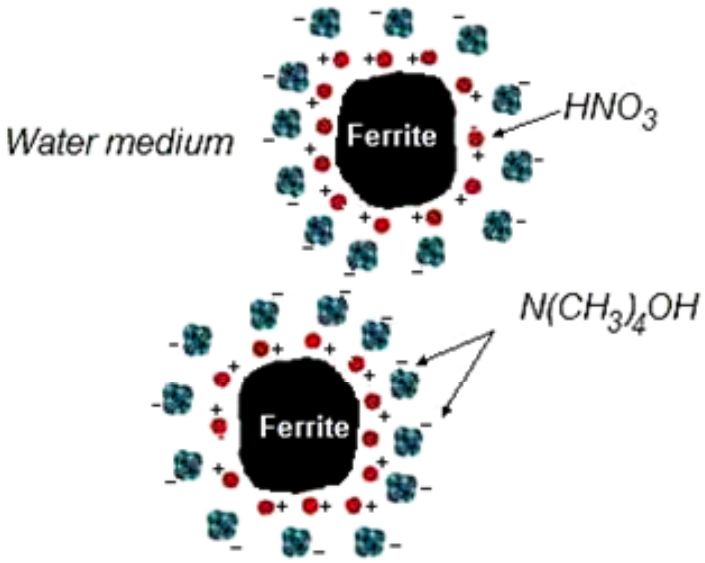

Figure 14: Double-layer surfactant coating of the particles

3.3 Numerical analysis of the coating effects of the wire

To better understand the effect of the coating of the wire in the experimental technique, a numerical model was developed. The objective of this analysis is to determine if the coating of the wire affects the outcome of the transient hot wire system, by solving numerically the line source problem with a coating layer over the source. Figure 15 shows the domain of integration of the problem, which is divided into three regions: Region 1, the platinum domain, Region 2, the coating domain and Region 3, the fluid domain. Since the interest is only on the initial transient, as has been explained before in the line source problem theory, natural convection can be neglected and the liquid is model as a solid.

Thermal properties are assigned to the domain, according to each one of these regions, and a harmonic mean conductivity is calculated at the region interfaces according to:

$$K_{e1} = \frac{2k_1k_2}{k_1k_2} \tag{3.4}$$

and

$$K_{e2} = \frac{2k_2k_3}{k_2k_3} \tag{3.5}$$

Where k_1, k_2 and k_3 are the thermal conductivities of the platinum, the coating and the liquid respectively.

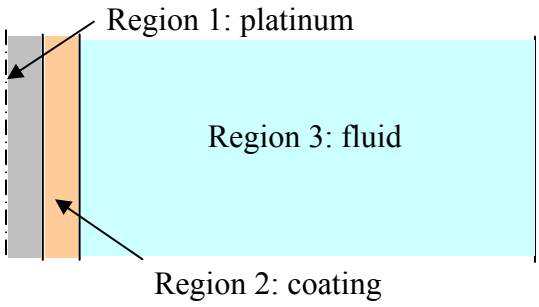

Figure 15: Domain of integration for the simulation

Figure 16 shows the temperature profile of a fluid medium around a continuous line heat source after six second. The fluid used for the simulation was water and the diameter of the line source was 62.5µm. It can be verified that there is not temperature profile in the y axis which means there are not bi-dimensional effects.

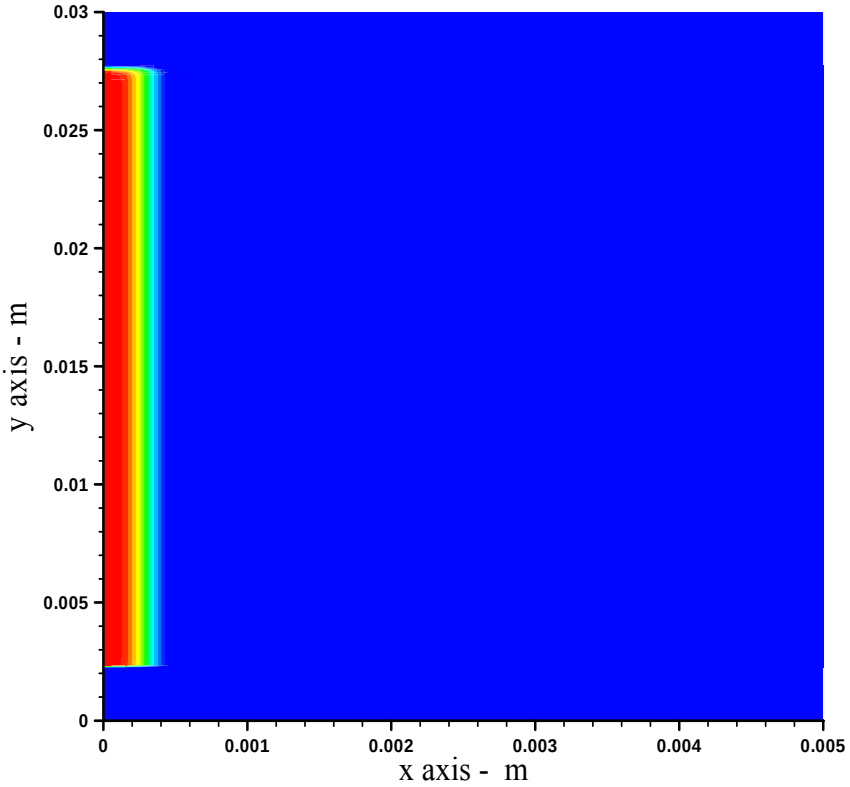

Figure 16: Temperature profile for Line source problem

From the 2D model, it was observed that bi-dimensional effects can be neglected if the length of the sensor is larger than 200 times the diameter of the sensor. Since this was the case in the experimental set up, a one dimensional model can be use for parametric studies of the effects of the coating in the temperature respond of the fluid. The governing equation is the conduction equation in cylindrical coordinates:

$$\rho C_p \frac{\partial \mathrm{T}}{\partial t} = \frac{k}{r}\frac{\partial}{\partial r}\left(r\frac{\partial T}{\partial r}\right) + \dot{q} \tag{3.6}$$

Here $\dot{q}$ is the volumetric heat generation in the sensor (the platinum region). *r* represents the radial axis, ρ is the density of the medium, depending on the region, and T is the temperature profile of the medium. The equation is discretized using a finite volume approach with a uniform grid size.

The main interest of this analysis is to investigate how the slope of the T vs. ln(time) line changes due to the presence of the coating. To understand the effect of the coating, some numerical experiments were carried out. Two different scenarios were considered: simulations with a coating and without a coating, for three different fluids (Mn0.7Zn0.3 Ferrofluid, water and methanol) and two coatings. Two different kind of coating will be used in the simulation to investigate how the answer is affected by the properties of the coating, especially by the thermal conductivity of the coating. The radius of the simulated sensor was 100 μm and the thickness of the coating 50 μm.

The thermal properties for $Mn_{0.7}Zn_{0.3}$ Fe_2O_4 ferrofluid used for the simulation were taken from the section 4.3.1. The properties of the three different fluids used for the simulation and the thermal properties used for the simulated coating are presented in table 4.

Table 3: Thermal properties of the fluids and the coatings used in the simulations

Media	ρ (kg/m3)	**Cp (**J/kg-K**)**	K (W/mK)
Water	1,000	4,180	0.6
Methanol	791	2,510	0.21
$Mn_{0.7}Zn_{0.3}$ ferrofluid	1,030	3,344	1.38
Coating 1	1,300	3,000	0.2
Coating 2	1,500	2600	0.9

Figure 17 shows the temperature of a point close to a continuous line source with coating and without coating for $Mn_{0.7}Zn_{0.3}$ Fe_2O_4 ferrofluid; with the time axis in a logarithmic scale. Also this figure shows that the presence of the coating does not change to much the temperature profile of the continuous line source, except at the initial 0.6 seconds. From the simulation can be confirmed the lineal relationship between the temperature and the ln(t) presented before for the analytical and for the experimental results.

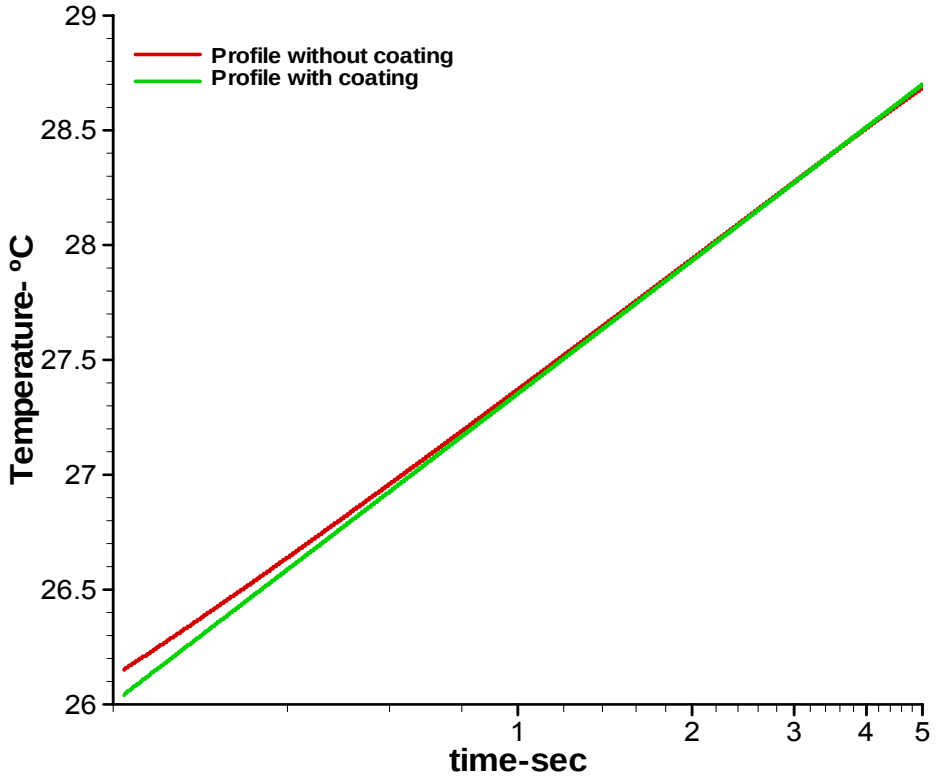

Figure 17: Temperature profiles for the $Mn_{0.7}Zn_{0.3}$ ferrofluid around a continuous line source with the coating 1 and without coating

Table 5 shows the calculated values of the slope $(T_2-T_1)/\ln(t_2/t_1)$, with the coating and without the coating, using the properties of the first coating (see table 4).The maximum deviation obtained was 4.03%. The slope with the coating was always smaller than the other one and the calculated values of the conductivity can be corrected with a correction constant due to the effect of the coating to reduce this difference.

Table 4: Simulation analysis for different fluids with the first coating

Media	Slope without coating	Slope with Coating	Deviation
Nanofluid	0.8362	0.8142	2.63%
Water	1.9229	1.8882	1.80%
Methanol	5.4945	5.2273	4.03%

Table 6 shows the calculated values of the slope $(T_2-T_1)/Ln(t_2/t_1)$, with the coating and without the coating, using the properties of the second coating (see table 4).The maximum deviation obtained was 4.39%. The slope with the coating was always smaller than the other one and the calculated values of the conductivity can be corrected with the correction constant mentioned before. Also it is evident that even for two different coatings with very different thermal properties the deviation between one and another slope remains being small.

Table 5: Simulation analysis for different fluids with the second coating

Media	Slope Without coating	Slope with Coating	Deviation
Nanofluid	0.8362	0.8137	2.69%
Water	1.9229	1.8383	4.39%
Methanol	5.4945	5.4212	1.33%

In the experiments, the effect of the coating is taking account by the calibration constant. Since the thickness of the coating will change due to degradation and delusion of the coating material, the calibration constant have to be recalculated before each set of measurements to avoid the usage of a wrong constant . However if the electrical insulation is lost, then errors in the estimation of the thermal conductivity are expected to be important.

4. RESULTS AND DISCUSSION

4.1 Nanoparticles characterization

Before the nanoparticles suspension in the fluid an analysis about the chemical composition and the crystallographic structure of the particles is performed. These results are presented in this section in order to verify the ferrite formation. A Siemens D500 diffractometer was used to confirm the formation of Mn-Zn ferrites crystalline structure and to determine the nanoparticle diameter (X-ray diffraction is a technique which reveal information about the crystallographic structure, chemical composition, and physical properties of materials based on observing the scattered intensity of an x-ray beam hitting a sample as a function of incident and scattered angle, polarization, and wavelength).

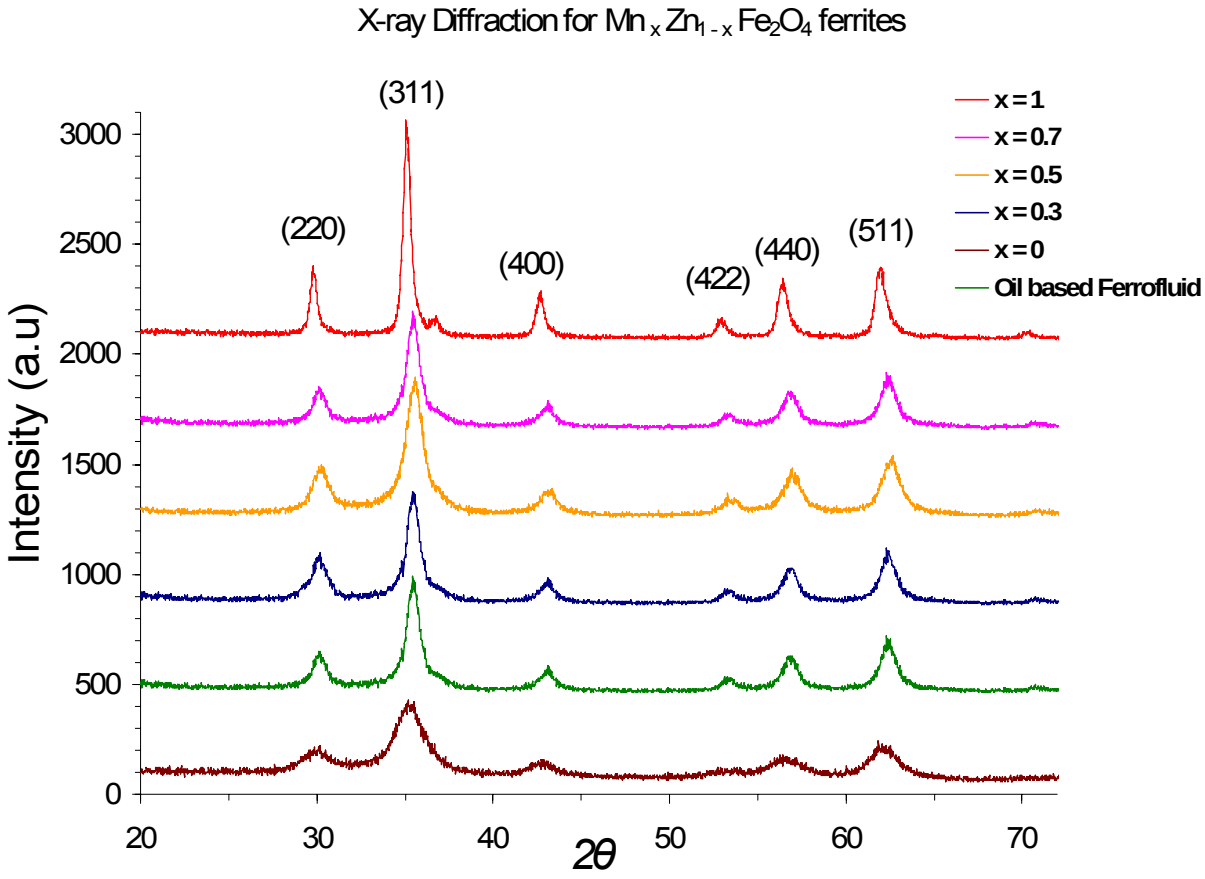

Figure 18: XRD pattern of Mn-Zn ferrites produced at different atomic fraction value 'x'

The XRD data for the solids particles produced by the synthesis as well as for the Mn-Zn ferrites particles of the oil-based ferrofluid (commercial ferrofluid) are presented in figure 18. In the figure different curves represent different Mn substitution values 'x' in the ferrite. As can be observed, for each one of the substitution ratios 'x' the structure is the same and all peaks correspond to a ferrite structure. The evidence of ferrite formation is corroborated when the (220), (311), (400), (422), (440) and (511) peaks appear in the x-ray diffraction pattern [36]. In addition, it is observed a small shifting in the peaks of the ferrites produced when the atomic ratio 'x' decreases from one to zero due to the zinc substitution in accordance with Almurugan [36].

For all the cases the Scherrer's equation was used to estimate the average crystallite size for different Mn substitution:

$$D_{avg} = \frac{K\lambda}{\beta \cos(\theta)} \tag{4.1}$$

Where K is the Scherer's constant (0.92), λ is the wavelength of the radiation and β is the integral breadth of the reflection. Table 3 shows the values obtained after X-ray diffraction for each atomic ratio 'x' value.

Table 6: Average crystallite size at different values of Mn substitution

X	Average crystallite Size (nm)
0	5.1
0.3	7.5
0.5	8.3
0.7	10.5
1	12.7
Oil-based ferrofluid	7.7

The higher is the atomic ratio "x" (bigger Mn amount), the larger is the average crystallite size, which is in good agreement with Auzans [37] and Calderon [15] works.

4.2. Estimation of volumetric concentration from magnetic measurements

In order to determine the volumetric concentration for the produced water-based Mn-Zn ferrofluid, a magnetic analysis (in addition of X-ray diffraction) was performed. Assuming monodispersity conditions, the particle diameter can be calculated by using the asymptotic values of the Langevin function as follows:

$$\frac{M}{\phi M_d} = \coth\alpha - \frac{1}{\alpha} = L(\alpha) \tag{4.2}$$

Where:

$$\alpha = \frac{mH}{k_B T} = \frac{\pi \mu_0 M_d H d^3}{k_B T} \tag{4.3}$$

M_d is the domain magnetization (bulk), m is the nanoparticles magnetic moment, μ_0 is the permeability of the free space ($4\pi x10^{-7} H/m$), T is the absolute temperature, k_B is the Boltzmann constant ($1.38x10^{-23} Nm/K$), H is the external magnetic field, and ϕ is the volume fraction. The initial susceptibility is given by $\chi_0 = \left.\frac{dM}{dH}\right|_{H\to 0}$. However, the magnetic properties of a ferrofluid are modified by the fact of particle size distribution; and then, the magnetization is given by the sum of the contributions for each particular diameter.

Using a weigh function to account for the particle size distribution; recalling that for large *H* values the relation between *M* and *1/H* should be a straight line crossing *M=0* axis at a point $1/H_0$ and applying a log normal distribution function the volumetric concentration for a ferrofluid having polydispersed nanoparticles according Chantrell [38] will be:

$$\phi = \frac{\chi_0}{3M_d H_0}\left[\frac{18k_B T}{\pi\mu_0 M_d d^3}\right]^2 \tag{4.4}$$

Where χ_0, $1/H_0$, d are determined experimentally and M_d is taken as 85emu/g for the produced ferrofluid [39].

From slope of the curve *M* vs *H* and *M* vs *1/H* for the ferrofluid for both low and high fields; at low fields the initial susceptibility value (χ_0) is obtained, while H_0 is obtained from the high field magnetic curve slope and the saturation magnetization value.

4.3 Thermal Characterization of Mn-Zn ferrofluids

The thermal conductivity of ferrofluids was measured using the transient hot wire method. All the experiments were carried out at room temperature and the temperature of the ferrofluid was the same for the sensor at the beginning of each experiment.

The quotient between the effective thermal conductivity of the ferrofluid K_{eff} and the thermal conductivity of the base fluid K_f was the parameter used to measure the increase in the thermal conductivity of the base fluid caused by the nanoparticles. This parameter was set as dependent variable respect to the volumetric concentration, the particle size, the base fluid and the chemical composition of the $Mn_xZn_{1-x}Fe_2O_4$ produced ferrofluids. The effect of each of those factors is presented and analyzed in the following sections in order to see how they are related to the change in the effective thermal conductivity of the base fluid when $Mn_xZn_{1-x}Fe_2O_4$ particles are suspended on it.

4.3.1 Analysis of the results by the crossed factor approach

A novel analysis is presented in which the effect of different factors that change the thermal conductivity of ferrofluids is analyzed by relating several factors instead of changing only one factor.

Using this analysis the one which affects the most to the change of the thermal conductivity can be identified. All the previous studies have been focused on the effects of a single factor affecting thermal conductivity. But thermal conductivity of ferrofluids is affected by different parameters and sometimes it is not possible to separate all of them and study their effect alone because by changing one, certainly changes other parameters.

For instance, if the volume concentration changes the surfactant needed to suspend the particles will change, increasing the pH of the solution and the surface potential of the suspended particles. Another possible case could be if the thermal conductivity of the particles changes by using another material, then another base fluid like ethylene glycol will be probably needed, changing the effective thermal conductivity of the ferrofluid.

$Mn_xZn_{1-x}Fe_2O_4$ ferrofluids are suitable to perform this kind of analysis since the atomic ratio 'x' is related to the particle diameter, and to the thermal conductivity of the nanoparticles. Also it is possible to observe the effect of the chemical composition of the particle in the effective thermal conductivity of the ferrofluid, since the atomic ratio permits to go from $ZnFe_2O_4$ to $MnFe_2O_4$ ferrofluid.

4.3.2 Effect of nanoparticle volumetric concentration "ϕ"

Figure 19 shows the lineal relationship between the volumetric concentration and the effective thermal conductivity for $Mn_{0.3}Zn_{0.7}Fe_2O_4$ water-based ferrofluid. The produced ferrofluid reported a variation from 0% to 34% of the effective thermal conductivity when increasing its volumetric concentration of nanoparticles from 0% to 3.12% for a 7.5nm average crystallite size.

Saturation condition was achieved for the ferrofluid when the volumetric concentration of nanoparticles reaches approximately 3.12%. For higher volumetric concentration the suspension process becomes very difficult, agglomeration occurs among the particles and

the particles settle down faster making almost impossible to stabilize the nanoparticles for a required long time.

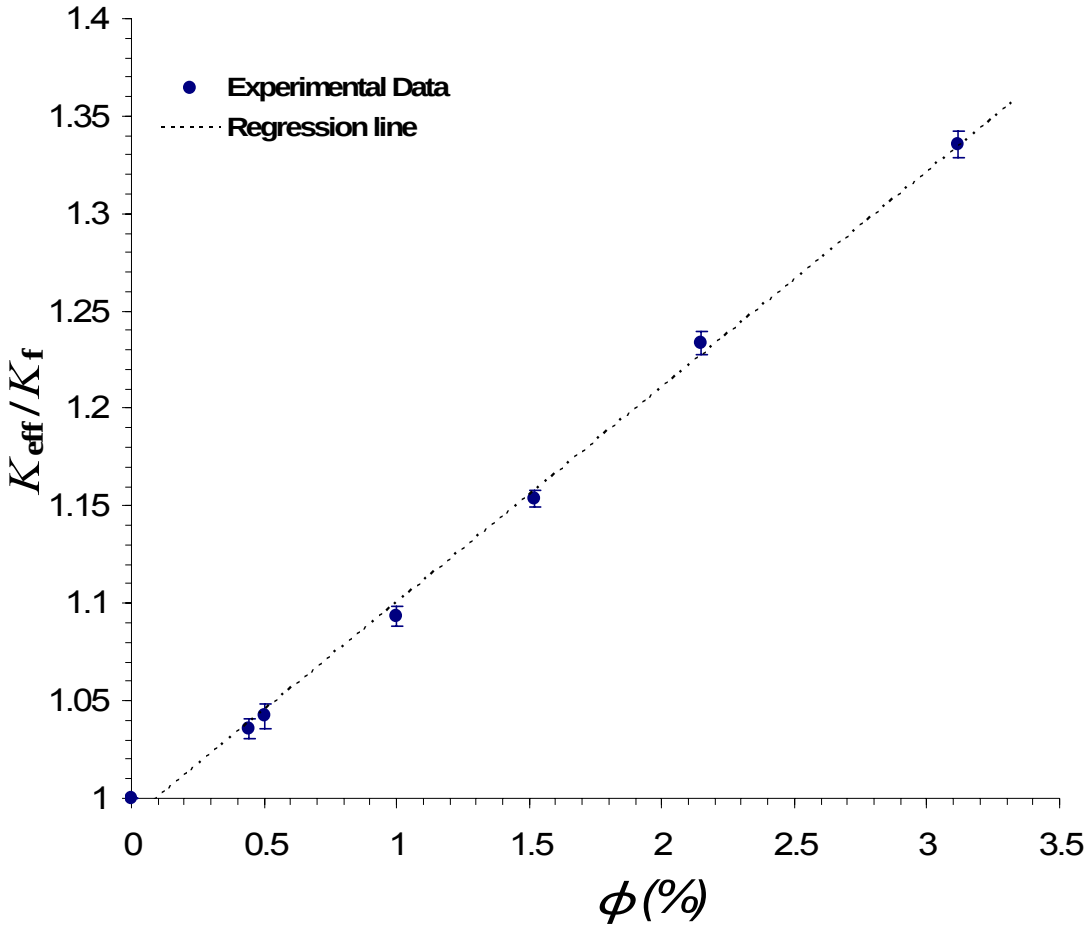

Figure 19: Thermal conductivity vs. volumetric concentration for $Mn_{0.3}Zn_{0.7}Fe_2O_4$ water-based ferrofluid

In order to see if the previous observed lineal behavior between the effective thermal conductivity and the volumetric concentration 'ϕ' is the same for different values of the atomic ratio 'x', the thermal conductivity of different ferrofluids from 0% to 3.12% was increased. Figure 20 shows the effective thermal conductivity of $Mn_xZn_{1-x}Fe_2O_4$ ferrofluids for atomic ratio varying from zero to one and for different volumetric concentration of nanoparticles.

The linear regression line established for each one of the data series almost fit exactly the experimental data for all the $Mn_xZn_{1-x}Fe_2O_4$ ferrofluids, demonstrating a linear dependence of the effective thermal conductivity of $Mn_xZn_{1-x}Fe_2O_4$ ferrofluids with the volumetric concentration of nanoparticles.

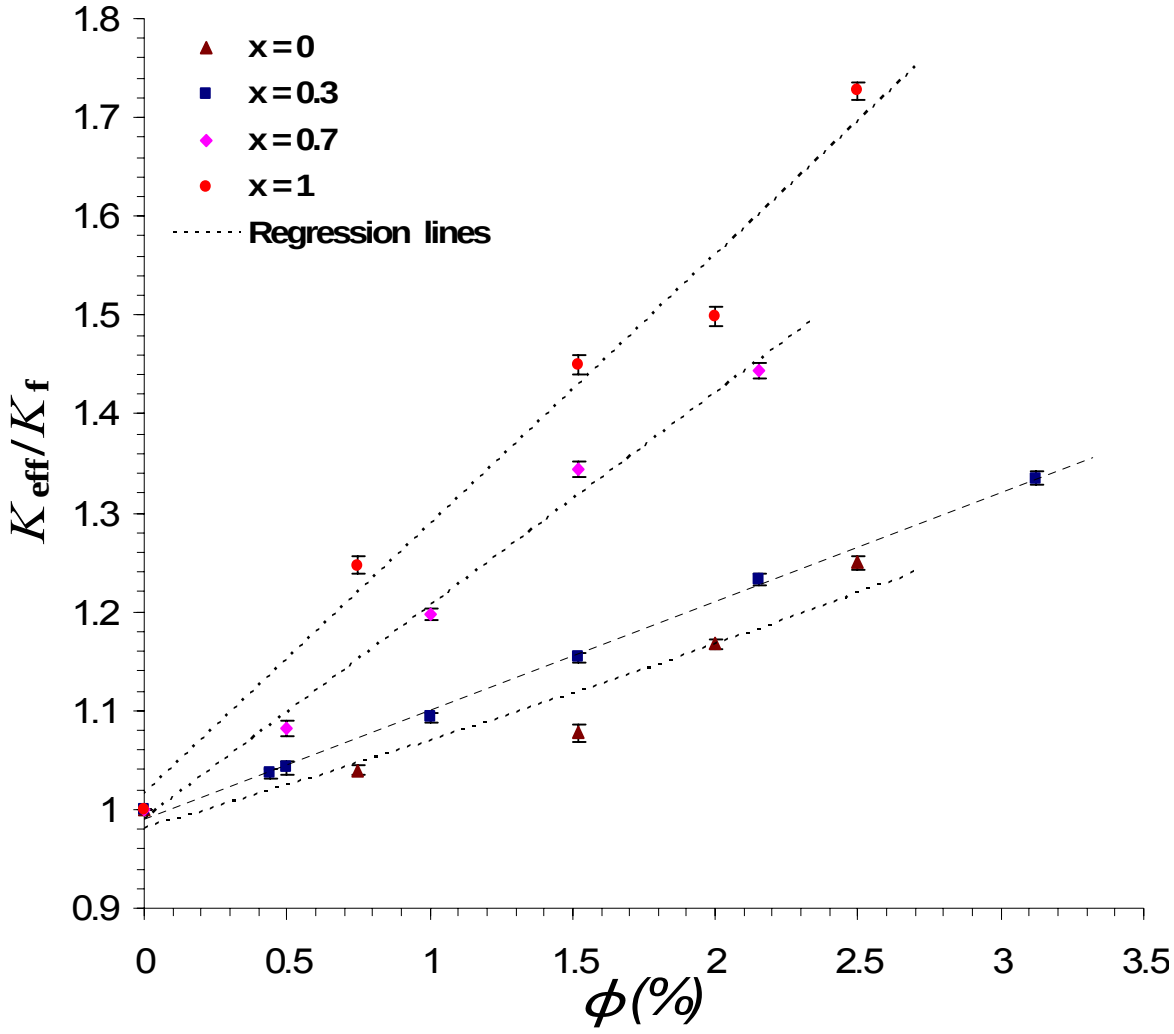

Figure 20: Thermal conductivity vs. volumetric concentration for $Mn_x Zn_{1-x} Fe_2 O_4$ water-based ferrofluids

A variation of 72% was the maximum increase reported in the effective thermal conductivity of ferrofluids. This case corresponds to $MnFe_2O_4$ ferrofluid when increasing the volumetric concentration of nanoparticles (12.67nm average crystallite size) from 0% to 2.5%.

Figure 20 shows a crossed factor case where volume concentration, particle diameter and chemical composition are related to the thermal conductivity. In this case the volumetric concentration can be analyzed alone because it is not related to the other two variables. From the figure 20 can be concluded that the influence of the particle diameter in the thermal conductivity of ferrofluids is higher than the influence of the thermal conductivity of the particles. Even when the thermal conductivity of the Zn is higher than the thermal conductivity of the manganese the thermal conductivity of the $MnFe_2O_4$ ferrofluid (x = 1) is higher than $ZnFe_2O_4$ ferrofluid (x = 0), due to the bigger particle diameter of the $MnFe_2O_4$ ferrofluid.

Also it can be observed that all the slopes of the regression lines are different, for instance with $ZnFe_2O_4$ ferrofluid the thermal conductivity enhancement rises 3.79% (K_{eff} /K_f changes from 1.0393 to 1.0772) when the volumetric concentration is doubled from 0.75% to 1.52% and with $MnFe_2O_4$ ferrofluid the thermal conductivity enhancement rises 20.22% (K_{eff}/K_f changes from 1.2472 to 1.4494) when the volumetric concentration changes in the same way. It can be concluded that volumetric concentration does not affect the effective thermal conductivity of all ferrofluids in the same way and although this two variables present a lineal relation, the slope of the line depends on other factors such as the particle diameter or the chemical composition of the particle.

4.3.3 Thermal conductivity and particle diameter

Thermal conductivity of ferrofluids is also influenced by the diameter and thermal conductivity of the nanoparticles. Figure 21 shows the effective thermal conductivity enhancement due to the particle diameter for different $Mn_xZn_{1-x}Fe_2O_4$ ferrofluids with a volumetric concentration of 1.52% for all the cases.

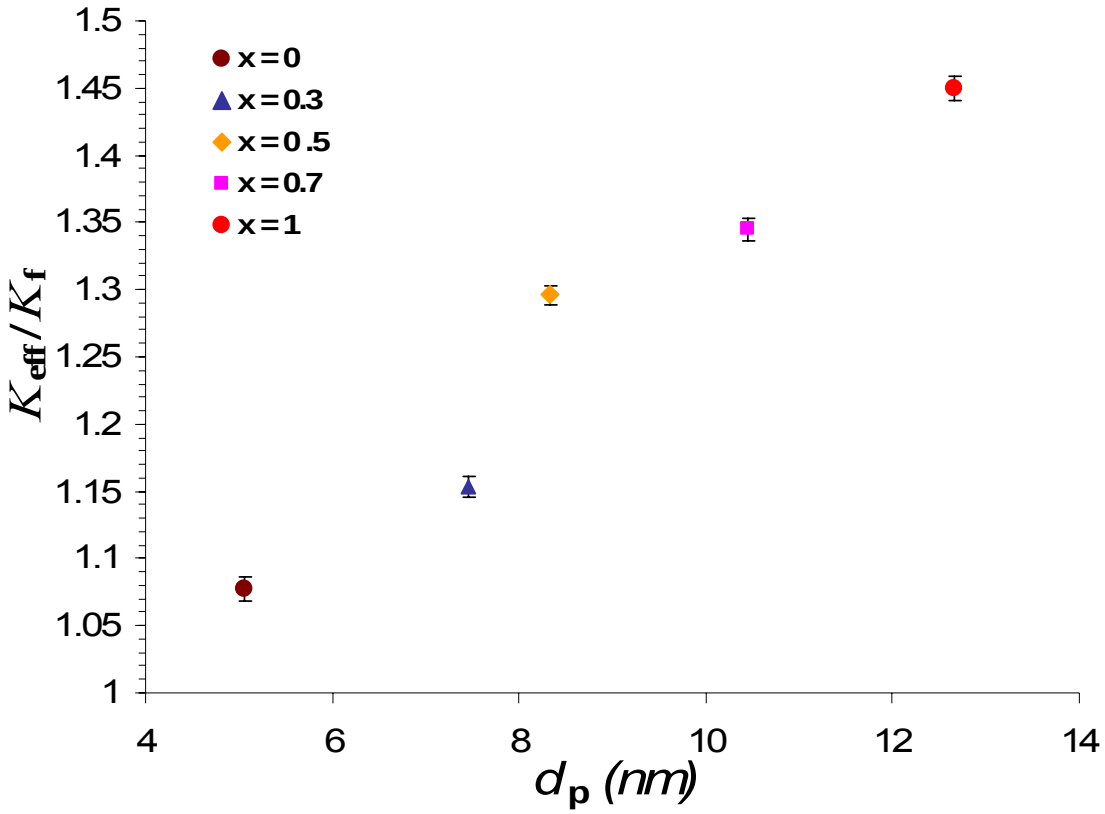

Figure 21: Thermal conductivity vs. average crystallite size for $Mn_xZn_{1-x}Fe_2O_4$ water-based ferrofluid

Figure 21 suggests a direct relation of the particle diameter with thermal conductivity for different $Mn_xZn_{1-x}Fe_2O_4$ ferrofluids with the same volumetric concentration. Although there is a clear dependency between the effective thermal conductivity and the particle diameter it is not exactly a lineal relation between these two variables.

Also, there is another variable that is influencing the relationship between the effective thermal conductivity and the particle diameter for this case. The atomic ratio 'x' is changing with the particle diameter from 0 to 1, making the effective thermal conductivity of the $Mn_xZn_{1-x}Fe_2O_4$ ferrofluid depend on the thermal conductivity of the nanoparticles also. The case of the crossed factors will be presented later in the following sections.

Figure 21 also shows a crossed factor effect where particle diameter and chemical composition are affecting effective thermal conductivity. In this case the volumetric concentration was fixed for all the fluids and the relation of the others two variables is more evident than in figure 20. From figure 21 it is arrived to the same previous conclusion that in figure 20.

4.3.4 Thermal conductivity and base fluid

Even when the absolute value of the thermal conductivity K_{eff} of the water-based $Mn_xZn_{1-x}Fe_2O_4$ ferrofluid is higher than the thermal conductivity of the $Mn_xZn_{1-x}Fe_2O_4$ oil-based ferrofluid; the K_{eff}/K_f parameter is higher for the oil-based ferrofluid. The reason why K_{eff}/K_f is higher is because the thermal conductivity of the base fluid is higher for water (0.6 W/mK) than for oils and common hydrocarbons (0.12-0.14 W/mK) frequently used as based fluid. Figure 22 shows the reported effective thermal conductivity for water-based $Mn_{0.3}Zn_{0.7}Fe_2O_4$ ferrofluid for three different volume concentrations from 1% to 3.12% and for oil-based $Mn_xZn_{1-x}Fe_2O_4$ ferrofluid for two different volume concentrations 1.02% to 2.04%.

Although the atomic ratio 'x' is unknown for the oil-based ferrofluid (commercial ferrofluid) the average crystallite size of nanoparticles is similar in both fluids (table 3).

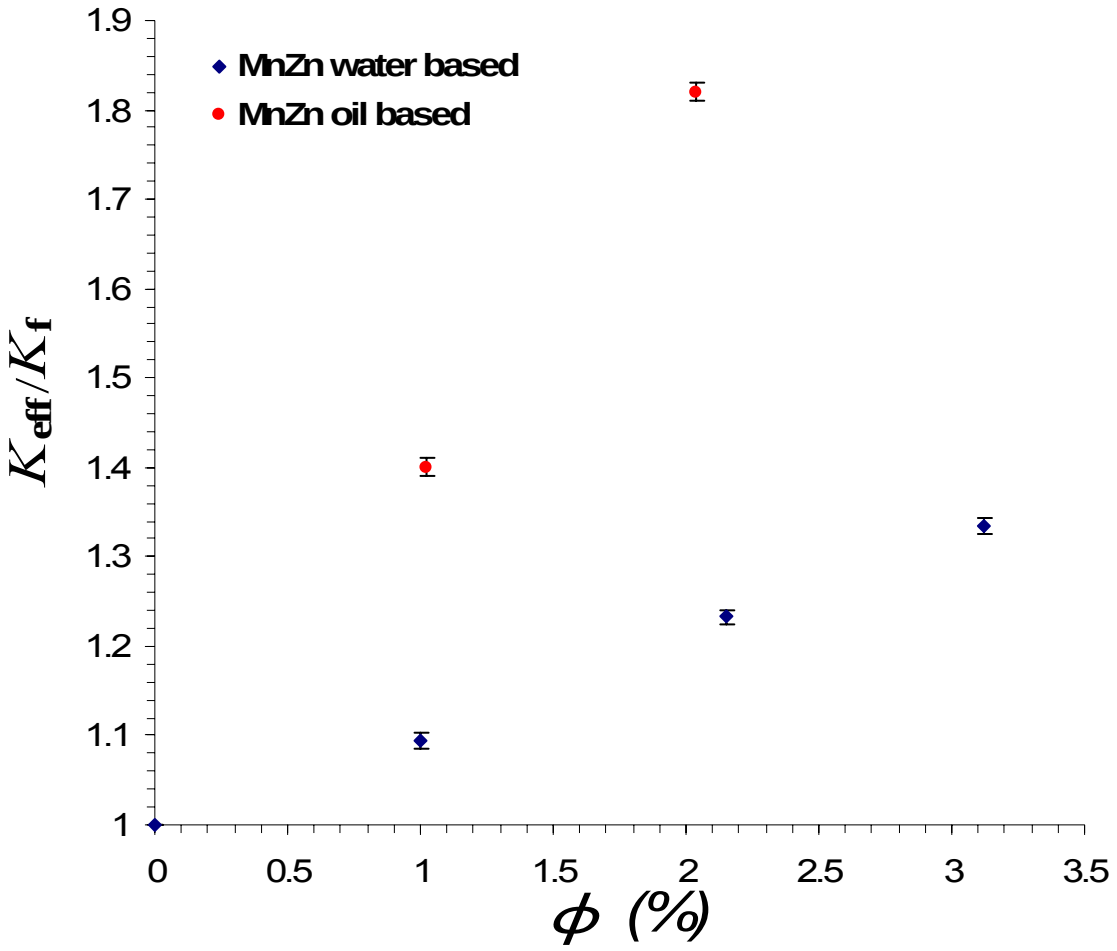

Figure 22: Thermal conductivity vs. base fluid for $Mn_x Zn_{1-x} Fe_2 O_4$ ferrofluids

The biggest value of the effective thermal conductivity for the water-based ferrofluid $K_{eff}/K_f = 1.34$ is lower than the smallest value of the effective thermal conductivity for the oil-based ferrofluid $K_{eff}/K_f = 1.4$. In spite of this fact, the absolute value of the thermal conductivity of the water-based ferrofluid $K_{eff} = 0.801$ W/mK is more than three times bigger than the absolute thermal conductivity of the oil-based ferrofluid $K_{eff} = 0.255$ W/mK for the highest volumetric concentration of both fluids.

4.3.5 Thermal conductivity and chemical composition

Preceding analyses suggest that chemical composition does not affect too much the increase of the effective thermal conductivity of ferrofluids. But it is inappropriate to arrive to that conclusion based only on the experimental results presented previously; since the observed increase was being affected by the particle diameter and the chemical composition at the same time. Therefore more experiments are needed in order to isolate the chemical composition influence of the nanoparticle on the thermal conductivity of ferrofluids.

Magnetite (Fe_3O_4) ferrofluid was chose to be compared with $ZnFe_2O_4$ ferrofluid due to the difference between the thermal conductivity of the Zinc and the Fe, in order to determine the chemical composition effect of the nanoparticle. The synthesis of Fe_3O_4 (magnetite) nanoparticle is performed using the same method used for the ferrite nanoparticle. But in this case Fe(II) is used as metal cation M(II).

Before suspending the nanoparticles in the fluid an analysis about the chemical composition and the crystallographic structure of the particles is performed. The XRD data for the solids particles produced by the synthesis are presented in figure 23 in order to verify the magnetite formation. The evidence of magnetite formation is corroborated when the (220), (311), (400), (422), (511) and (440) peaks appear in the x-ray diffraction pattern. The average crystallite size of the magnetite nanoparticles was estimated using again the Scherrer's equation and it was found to be 6.1 nm.

It is important to note that the average crystallite size for both ferrofluid nanoparticles is very similar, 6.1 nm for the magnetite and 5.1 nm for the Zn ferrite. Then if the ferrofluids are compared for the same volumetric concentration, the chemical composition effect over the thermal conductivity of ferrofluids will be isolated.

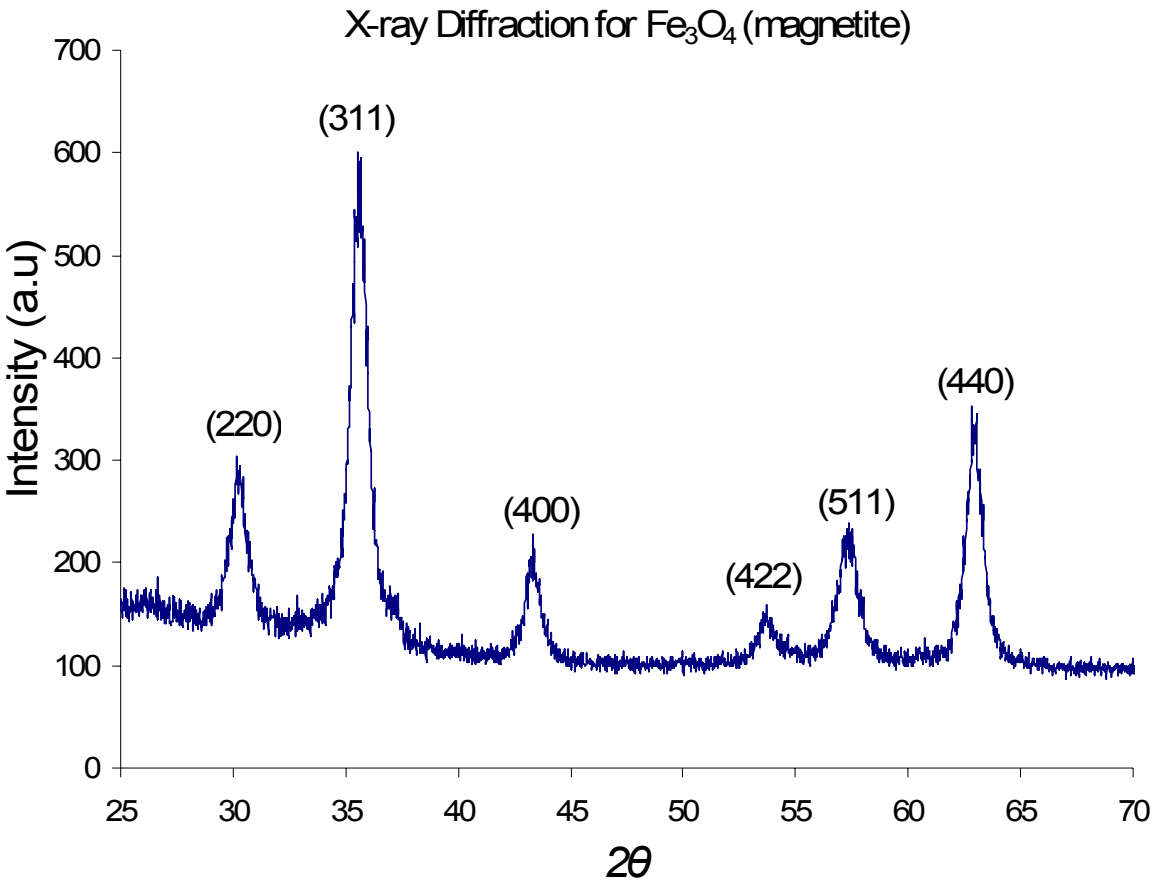

Figure 23: XRD pattern of magnetite

Magnetite ferrofluid preparation was performed using the same technique presented before for ferrite ferrofluid preparation. Also Magnetite ferrofluid was prepared using the same volumetric concentrations of the ferrites in order to analyze only the influence of the chemical composition on the effective thermal conductivity of ferrofluid.

Figure 24 shows the lineal relationship between the volumetric concentration and the effective thermal conductivity for $ZnFe_2O_4$ and Fe_3O_4 water-based ferrofluid. The produced ferrofluid reported a variation from 0% to 25% of the effective thermal conductivity when increasing its volumetric concentration of nanoparticles from 0% to 2.5% for a similar average crystallite size.

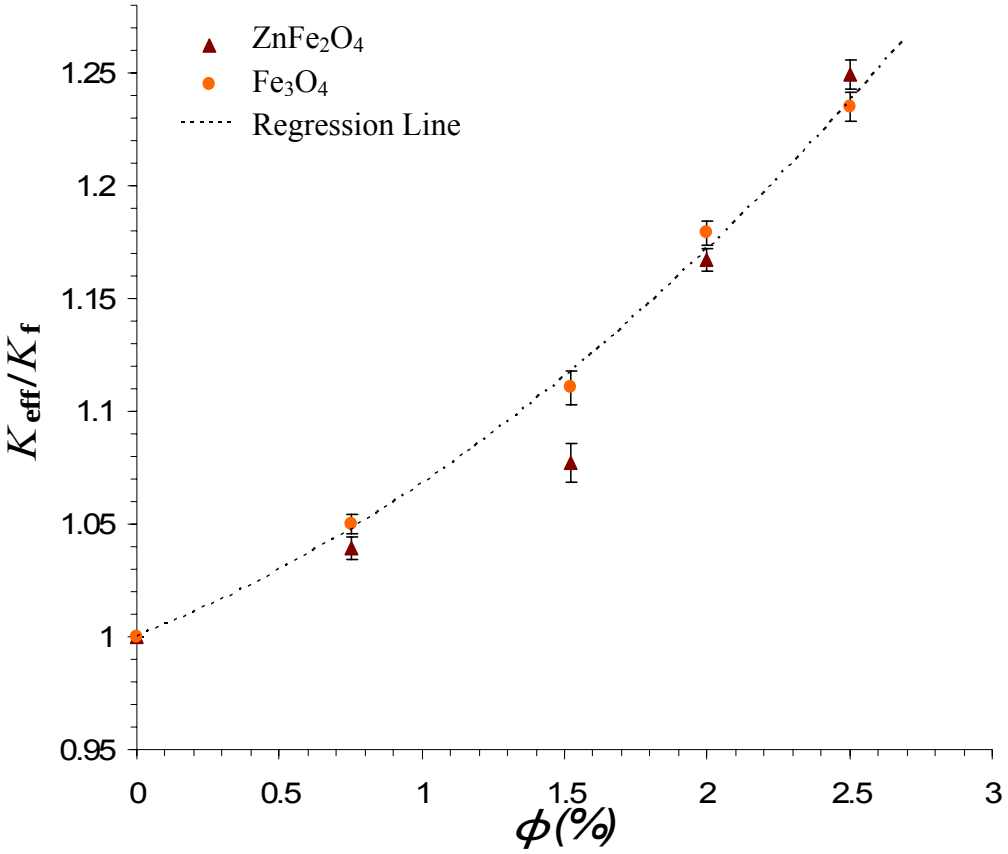

Figure 24: Thermal conductivity vs. volumetric concentration for $ZnFe_2O_4$ and Fe_2O_3 water-based ferrofluids

Also figure 24 shows that the chemical composition of the nanoparticles does not affect the effective thermal conductivity of ferrofluids. Since for the same volumetric concentration and almost the same particle diameter the effective thermal conductivity of both ferrofluids is almost the same for all the cases.

In figure 25 the lineal dependence of the effective thermal conductivity on the volumetric concentration of nanoparticle is presented. For all the ferrofluids the tendency to increase the thermal conductivity by increasing the volumetric concentration of nanoparticles is observed. Also figure 25 shows that the effective thermal conductivity of magnetite is smaller than the effective thermal conductivity of $Mn_{0.3}Zn_{0.7}$ Fe_20_4 ferrofluid for all the volumetric concentration value. The same tendency was observed in figure 20 for $ZnFe_20_4$ ferrofluid, suggesting in that way that the effective thermal conductivity is not affected too much by the chemical composition of the nanoparticle.

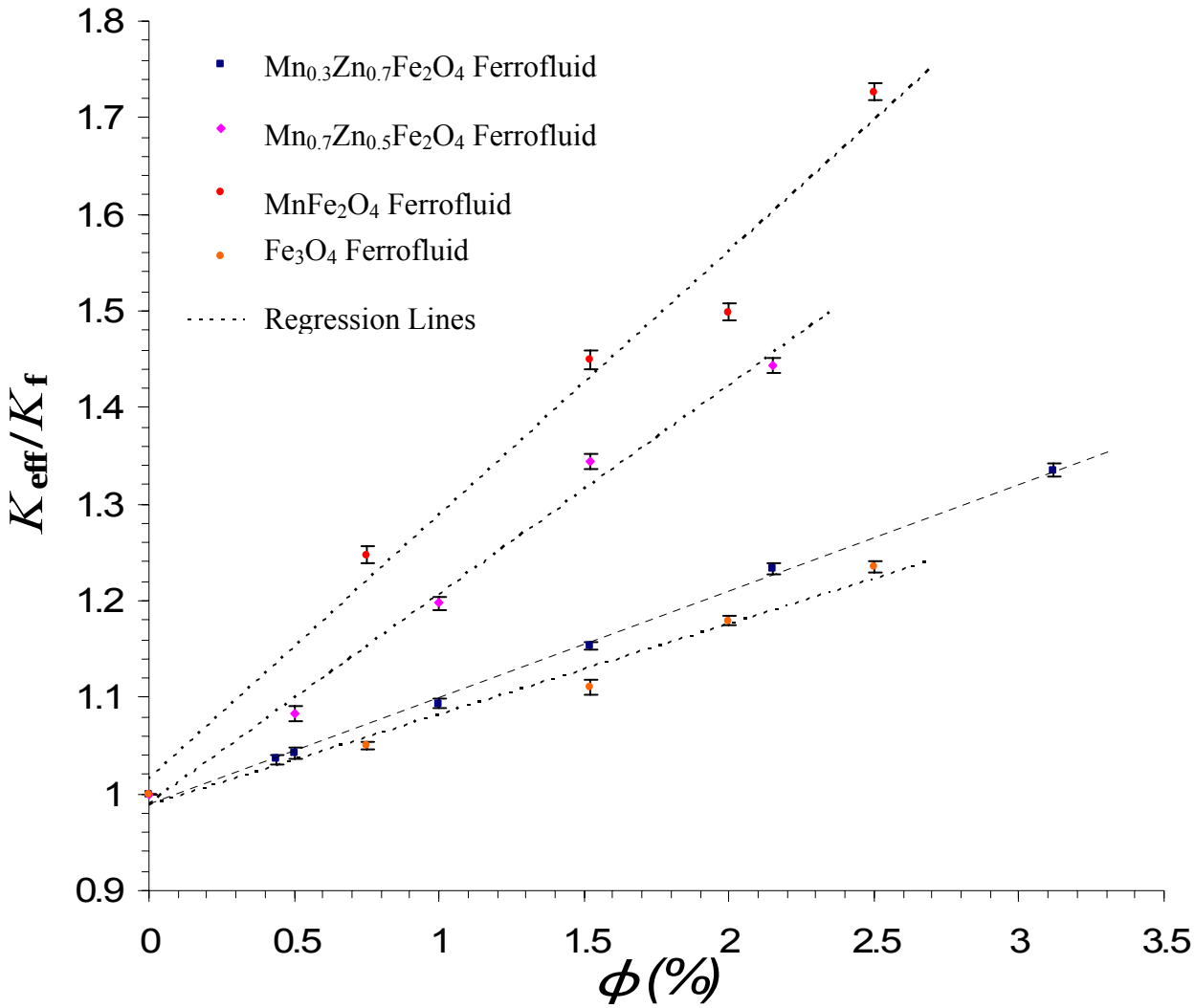

Figure 25: Thermal conductivity vs. volumetric concentration for different water-based ferrofluids

5. CONCLUSIONS AND RECOMENDATIONS

A transient hot wire system capable to measure the thermal conductivity of fluids was designed and used to characterize different ferrofluids. All the nanofluids analyzed here have shown an enhancement in the thermal conductivity. $Mn_xZn_{1-x}Fe_2O_4$ ferrofluids showing great potential for heat transfer applications, presenting in some cases a 70% increase on its thermal conductivity for less than 3% volumetric concentration of particles.

The influence of some important parameters on the thermal conductivity has been studied. The volumetric concentration of nanoparticles in the ferrofluid was found to be a key aspect of the thermal performance of a ferrofluid. In strong agreement with literature a lineal relationship between the effective thermal conductivity of the ferrofluids and the volumetric concentration of nanoparticles was observed on the experimental results.

A higher effective thermal conductivity was found in ferrofluids with higher particle diameter. Using the proposed cross factor analysis has been shown that the particle size is more important factor than the thermal conductivity of the nanoparticle in the enhancement of the effective thermal conductivity of the ferrofluids. Also the particle diameter was found to be more important than the chemical composition of the particle, since the thermal conductivity of two different particles with almost the same particle diameter was found to be almost the same.

The coating effect of the wire in the outcome of the transient hot wire system has been analyzed by solving numerically the heat equation for the line source case. It has been shown that the coating does not affect too much the results of the measurements and a calibration constant must be used to diminish the error in the measurement of the effective thermal conductivity.

However it is very important to provide an electrical insulation to the platinum wire, in order to obtain appropriate values of thermal conductivity of an electrical conductive fluid. Because, if the electrical current in the wire flows throw the fluid, the applied electric power "*q*" becomes uncertain to determine.

To a better understanding of the contribution of the particle diameter, it is recommended the realization of new measurements in order to separate the effects of the particle diameter and the chemical composition of the particles. Also it is recommended to consider the influence of the surface chemical effect of the particle on the thermal conductivity enhancement of ferrofluids.

APPENDIX

The continuous line source problem

In this section a detailed analysis about the theory behind the transient hot wire method is presented, in which the key feature is the generation of heat in a very small region – a concentrated source- of the conducting medium. The small region, the wire in the transient hot wire apparatus, will be modeled by mean of a straight line. When heat is released into the medium from this line, the process will be a transient conduction problem in the surrounding area of a heat source.

The solution for the instantaneous point source will be taken as a fundamental solution. By integrating with respect to the appropriate space variable, the solution for an instantaneous line source problem is obtained. Then by integration with respect to time the solution for the continuous line source is obtained, corresponding to the release of heat at a given line at a prescribed rate *Q (t)* per unit time. The equation of heat conduction, when expressed in spherical polar coordinates, becomes:

$$\frac{\partial T}{\partial t} = \alpha\left\{\frac{1}{r^2}\frac{\partial}{\partial r}\left(r^2\frac{\partial T}{\partial r}\right) + \frac{1}{r^2\sin\theta}\frac{\partial}{\partial\theta}\left(\sin\theta\frac{\partial T}{\partial\theta}\right) + \frac{1}{r^2\sin^2\theta}\frac{\partial^2 T}{\partial\phi^2}\right\} \qquad \text{(A.1)}$$

In the limit of the actual case, in which a finite quantity of heat is liberated over a vanishingly small volume, suppose that volume is a sphere of radius *a*, and consider the case of an infinite medium with constant properties (k, ρ, α, c), in which the initial temperature is T_o in the sphere $0 \le r < a$ and zero in the region $r > a$. The heat equation now is:

$$\frac{\partial T}{\partial t} = \alpha\left(\frac{\partial^2 T}{\partial r^2} + \frac{2}{r}\frac{\partial T}{\partial r}\right) \qquad \text{(A.2)}$$

On putting $U = Tr$, the equation become:

$$\frac{\partial U}{\partial t} = \alpha \frac{\partial^2 U}{\partial r^2} \tag{A.3}$$

With the following initial and boundary conditions:

$U = T_o r$, when $t \leq 0$, $0 < r < a$, $\quad U = 0$, when $r \to \infty$

$U = 0$, when $t \leq 0$, $r > a$ $\quad \frac{\partial U}{\partial r} = 0$ when $r = 0$

The approximate solution assuming a small radius is:

$$T(r,t) = \frac{Q}{8\rho c(\pi\alpha t)^{3/2}} \exp\left(\frac{-r^2}{4\alpha t}\right)\left\{1 + \frac{1}{t}\left(\frac{r^2 a^2}{40\alpha^2 t} - \frac{6a^2}{40\alpha}\right)\right\} \tag{A.4}$$

Now in order to analyze the point source let the radius of the sphere tend to zero. If the term 1/t is small enough and Q remaining constant equation (A.4) becomes:

$$T(r,t) = \frac{Q}{8\rho c(\pi\alpha t)^{3/2}} \exp\left(\frac{-r^2}{4\alpha t}\right) \tag{A.5}$$

This equation describes the temperature history near an instantaneous point source, where Q is the heat transfer to de medium in joule at time $t=0$, and the radial distance r is measured away from the point source $(r = 0)$. Now, in order to obtain the solution for an instantaneous line source, a distribution of instantaneous point sources of strength $Q\,dz$ at $t=0$ will be consider, parallel to the z axis and passing through the origin of the coordinate system.

$$T(r,t) = \frac{Q}{8\rho c(\pi\alpha t)^{3/2}} \int_{-\infty}^{\infty} \exp\left(\frac{-r^2}{4\alpha t}\right) dz \tag{A.6}$$

The temperature obtained after the integration of equation (A.6) is:

$$T(r,t) = \frac{Q'}{4\rho c \pi \alpha t} \exp\left(\frac{-r^2}{4\alpha t}\right) \tag{A.7}$$

In this expression Q' is the strength of the instantaneous line source, that is, the heat per unit length *(J/m)* that is release only once at $t=0$. The radial distance r is measured away from the line source. Finally the temperature for the continuous line source has to be determined.

The time-dependent temperature distributions and conduction processes that are induced by sources that persist on time can be determined analytically by superposing the effect of a large number of instantaneous sources. In the superposition procedure each one-shot heat source Q' (Joule per unit length) takes place in the presence (on the background) of the temperature profile created by a previous shot at a preceding time interval. Then the temperature distribution after any time t is simply the sum of all the temperature distributions that results after each shot of Q' released before t. A continuous line source has the same effect as a sequence of very large number of small instantaneous line sources of equal size:

$$\Delta Q' = q'' \Delta t \tag{A.8}$$

Where q'' *(W/m)* is the heat transfer deposited per unit length per unit time, and Δt is the short duration of each shot. As Δt becomes infinitesimally small, the number of terms in the finite-time interval sum of all the temperature distributions, become infinite, and the sum is replaced by the integral:

$$T(r,t) = \frac{q''}{4\rho c \pi \alpha} \int_0^t \exp\left(\frac{-r^2}{4\alpha(t-t')}\right) \frac{dt'}{t-t'} \tag{A.9}$$

Under the integral sign, the dummy variable t' marks the time when each additional instantaneous source $q''dt'$ springs into action. Changing the variable of the integration by $u = r^2 / 4\alpha (t - t')$ the equation become:

$$T(r,\, t') \;=\; -\frac{q''}{4\rho c \pi \alpha}\; Ei\left(-\frac{r^2}{4\alpha t}\right) \tag{A.10}$$

Where $Ei(x)$ is the exponential integral function and is defined as:

$$-\; Ei\,(-x) \;=\; \int_x^{\infty} \frac{\exp\,(-\,u\,)}{u} du \tag{A.11}$$

For the small values of *x,* $Ei(x)$ can be represented as:

$$Ei(-x) = \gamma + \ln(x) - x + \frac{1}{4}x^2 + \frac{1}{18}(x^3) \tag{A.12}$$

Where γ = 0.577216 is the Euler's constant. The exponential integral can be evaluated and the resulting expression is the temperature distribution near *r=0* line in which the continuous source *q"* is turned on at t=0. At sufficiently long times and/or small radial distance, where the group $r^2/4\alpha t$ is smaller than 1, the temperature profile is:

$$T(r,t) = \frac{q''}{4\pi k}\left[\ln\left(\frac{4\alpha t}{r^2}\right) - \gamma\right] \qquad \left(\frac{r^2}{4\alpha t}\right) << 1 \tag{A.13}$$

This solution is of great importance. It gives the temperature in an infinite solid which is heated along a line; say by an ideally thin wire carrying electric current. Thus is an approximation to the heating of an infinite solid by a wire carrying current because it is considered that the term 1/t of equation (A.4) was small enough to be negligible.

If there is a contact resistance R per unit length between the wire and the surrounding medium and considering the effect of the finite radio (a) of the wire it is obtained that the temperature on the surface of the wire is [8]:

$$T(\tau) = \frac{q''}{4\pi k}\left\{2h + \ln\left(\frac{4\tau}{e^{\gamma}}\right) - \frac{(4h-\vartheta)}{2\vartheta\tau} + \frac{\vartheta-2}{2\vartheta\tau}\ln\left(\frac{4\tau}{e^{\gamma}}\right)\right\} \qquad \text{(A.14)}$$

Where: $h = 2\pi Rk$, $\vartheta = 2a^2\pi\rho c/S$, $\tau = kt/a^2$ and S is the thermal capacity of the wire per unit length.

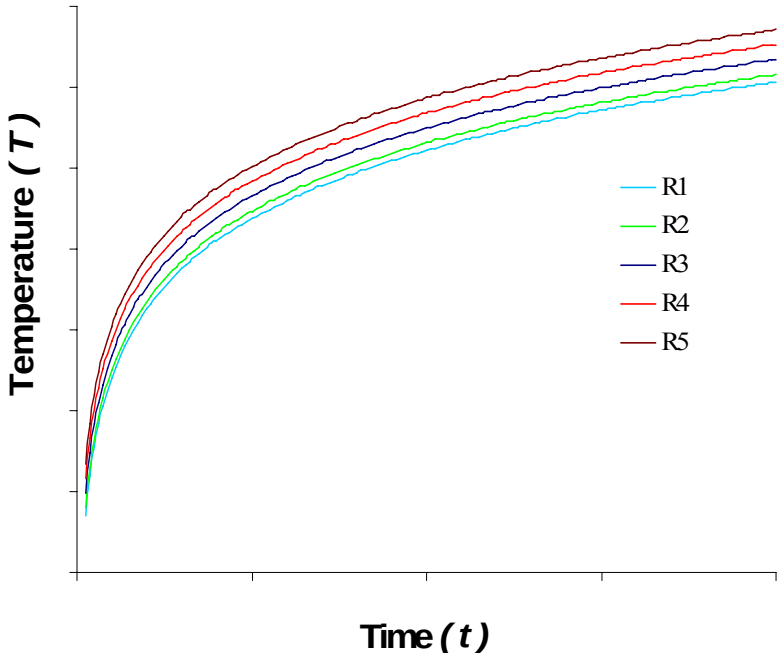

Figure 26: Line source temperature for different values of R

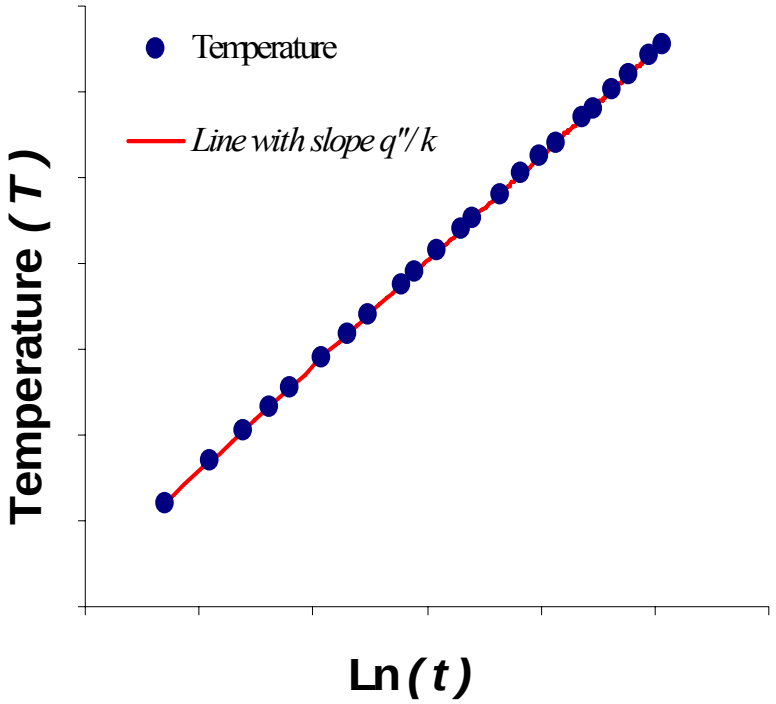

Figure 27: Lineal behavior of T vs. ln(t)

Figure 3-b shows the lineal behavior of T vs. *ln(t)* for $R=R1$. It follows from equation (A.14) and from figure 3 that in all cases for different values of R, a curve of T against *ln(t)* has a linear asymptote of slope q''/k, and thus if q'' is known, k is determined immediately.

REFERENCES

[1] J. C. Maxwell, A Treatise on Electricity and Magnetism, second ed., Claredon Press, Oxford, UK, 1881.

[2] S. U. S. Choi, Enhancing Thermal Conductivity of Fluids with Nanoparticles, Developments and Applications of Non-Newtonian Flows, FED-vol.231/MD-vol.66, 1995, pp. 99-105.

[3] S. K. Das, N. Putra, P. Thiesen, and W. Roetzel, Temperature dependence of thermal conductivity enhancement for nanofluids, Journal of Heat Transfer, vol. 125, 2003, pp. 567-574.

[4] M. S. Liu, M. C. Lin, C. Y. Tsai and C. C. Wang, Enhancement of thermal conductivity with Cu for nanofluids using chemical reduction method, Int. Journal of Heat and Mass Transfer, vol.49, 2006, pp. 3028–3033.

[5] C. Wu, B. P. Mosher and T. Zeng, One-step green route to narrowly dispersed copper nanocrystals, Journal of nanoparticles research, vol. 8, No. 6, 2006, pp. 965-969.

[6] J. G. Webster, The Measurement, Instrumentation and Sensors Handbook, CRC press LLC, US, 1999, pp.33-4.

[7] S.K. Das, N. Putra, P. Thiesen, W. Roetzel, Temperature dependence of thermal conductivity enhancement for nanofluids, J. Heat Transfer,Vol. 125, 2003, pp. 567–574.

[8] H.S. Carslaw and J. C. Jaeger, Conduction of Heat in Solids (Oxford U. P., Oxford), 1959, pp. 256-262,341-345.

[9] Y. Xuan and Q. Li, Heat transfer enhancement of nanofluids. Int. J. of Heat and Fluid Flow, vol.21, 2000, pp. 58-64.

[10] S. U. S. Choi, Z. G. Zhang, W. Yu, F. E. lockwood, and E. A. Grulke, Anomalous thermal conductivity enhancement in nano-tube suspensions. Appl. Phys. letters. vol. 79, 2001, pp. 2252-2254.

[11] Y. Nagasaka, and A. Nagashima, "Absolute Measurement of the Thermal Conductivity of Electrically Conducting Liquids by the Transient Hot-wire Method," Journal of Physics E: Scientific Instruments Vol. 14, 1981, pp. 1435-1440.

[12] X. Wang, X. Xu, S.U.S. Choi, Thermal conductivity of nanoparticle–fluid mixture, Journal of Thermophysics and Heat Transfer, Vol. 13, No. 4, 1999, pp. 474–480.

[13] D. Zins, R. Massart, E. Auzans, E. Blums, Synthesis and Properties of Mn-Zn Ferrite Ferrofluids, Journal of Material Science, Vol. 34, 1999, pp. 1253-1260.

[14] E. Calderon, - $Mn_xZn_{1-x}Fe_{2-Y}R_YO_4$ (R = GD, EU) ferrite nanocrystals for potential magnetocaloric applications, ENS-1030Technical publication, Proceedings of European Nano System, December 2007.

[15] L.J Love, J.F. Jansen, T.E. Mcknight, Y. Roh, T.J.A Phelps, A Magnetocaloric Pump for Microfluid Applications, IEEE Transactions on nanobioscience. Vol. 3, No. 2, 2004

[16] J.E. Cataño, O. Perales, M. Tomar, E. Calderon, And C. Melendez, Characterization of Mn-Zn magnetic fluid for cooling applications at ambient temperature. Technical publication, ASME, Proceedings of IMECE November 2005.

[17] J.A. Eastman, U.S. Choi, S. Li, L.J. Thompson, S. Lee, Enhanced thermal conductivity through the development of nanofluids, Materials Research Society Symposium – Proceedings, vol. 457, Materials Research Society, Pittsburgh, PA, USA, Boston, MA, USA, 1997, pp. 3–11.

[18] S. Lee, S.U.S. Choi, S. Li, J.A. Eastman, Measuring thermal conductivity of fluids containing oxide nanoparticles, Journal of Heat Transfer Vol. 121, 1999, pp. 280–289.

[19] Eastman, J. A.; Choi, S. U. S.; Li, S.; Yu, W.; Thompson, L. J. Anomalously increased effective thermal conductivities of ethylene glycol-based nanofluids containing copper nanoparticles, Appl. Phys. Lett., 2001, Vol. 78, No. 6, pp. 718-720.

[20] S.M.S. Murshed, K.C. Leong, C. Yang, Enhanced thermal conductivity of TiO_2–water based nanofluids, International Journal of Thermal Sciences Vol. 44, No. 4, 2005, p 367.

[21] T.-K. Hong, H.-S. Yang, C.J. Choi, Study of the enhanced thermal conductivity of Fe nanofluids, Journal of Applied Physics Vol. 97, No. 6, 2005, pp. 1–4.

[22] C-W. Nan, R. Birringer, D. R. Clarke and H. Gleiter, Effective Thermal conductivity of Particulate Composites With Interfacial Thermal Resistance, J. Appl. Phys., Vol. 81, 1997, pp. 6692–6699.

[23] O. M. Wilson, Xiaoyuan Hu, D. G. Cahill, and P. Braun, Colloidal Metal Particles as Probes of Nanoscale Thermal Transport In Fluids, Phys. Rev. B., Vol. 66, 2002, pp. 224301-1 – 224301-5.

[24] S.T. Huxtable, D.G. Cahill, S. Shenogin, L. Xue, R. Ozisik, P. Barone, M. Usrey, M.S. Strano, G. Siddons, M. Shim, P. Kebunski, Interfacial Heat Flow in Carbon Nanotube Suspensions, Nat. Mater. Vol. 2, 2003, pp.731–734.

[25] D.A.G. Bruggeman, Berechnung Verschiedener, Physikalischer Konstanten von Heterogenen Substanzen, I Dielektrizitatskonstanten und Leitfahigkeiten der Mischkorper aus Isotropen Substanzen. Annalen der Physik. Leipzig, Vol. 24, 1935, pp. 636–679.

[26] R.L. Hamilton and O.K. Crosser, Thermal conductivity of heterogeneous two component systems, I&EC Fundam 1, 1962, pp. 182–191.

[27] Y. Xuan, Q. Li, W. Hu, Aggregation structure and thermal conductivity of nanofluids, AIChE Journal Vol. 49 ,No.4, 2003, pp. 1038–1043.

[28] J. Koo, C. Kleinstreuer, A new thermal conductivity model for nanofluids, Journal of Nanoparticle Research, Vol. 6 No.6, 2004, pp. 577–588.

[29] Q. Xue, W.-M. Xu, A model of thermal conductivity of nanofluids with interfacial shells, Materials Chemistry and Physics, Vol. 90 No.2–3, 2005, pp.298– 301.

[30] P. Keblinski, S. R. Phillpot, S. U. S. Choi, J. A. Eastman, Mechanisms of Heat Flow in Suspensions of Nano-sized Particles (Nanofluids), Int. J. Heat Mass Transfer, 2002, Vol. 45, pp. 855–863.

[31] C. J. Yu, A. G. Richter, A. Datta, M. K. Durbin, P. Dutta, Molecular layering in a liquid on a solid substrate: an X-ray reflectivity study, Physica B, 2000, Vol.283, pp. 27-31.

[32] R. Prasher, P. Bhattacharya, P.E. Phelan, Brownian-motion-based convective-conductive model for the effective thermal conductivity of nanofluids, J. Heat Transfer, Vol. 128, 2006, pp. 588–595.

[33] D. Lee, J-W. Kim, B. Kim, A new parameter to control heat transport in nanofluids: surface charge state of the particle in suspension, J. Phys. Chem. B, 2006, Vol. 110, pp. 4323-4328.

[34] L. Xue et al. L. Xuea, P. Keblinski, S. R. Phillpot, S. U. S. Choi and J. A. Eastman, Two regimes of thermal resistance at a liquid-solid interface, J. Chem. Phys., 2003, Vol. 118, pp. 337-339.

[35] T. Beckwith, R. Marangoni, and J. Lienhard, Mechanical Measurements, Addison Wesley, Reading, MA. 1993.

[36] R. Almurugan, G. Vaidyanatahan, S. Sendhilnatan, B. Jadevayan. Effect of Zinc substitution on C0-Zn and Mn-Zn ferrite nanoparticles prepared by co-precipitation, Journal of Magnetism and Magnetic Materials, 288 (2005) 470-477

[37] E. Auzans. Mn-Zn ferrite nanoparticles for water- and hydrocarbon-based ferrofluids: preparation and properties. Institute of Physics of Latvian University. PHD Thesis, 1999.

[38] R.W Chantrell, J. Popplewell and S.W Charles. Measurements of Particle Size Distribution Parameters in Ferrofluids. IEEE transactions on magnetics, Vol. MAG-14 No. 5, 1978

[39] E. Bermudez, Design and mechanical characterization of a magnetocaloric pump, Mechanical Engineering, University of Puerto Rico at Mayaguez, MS Thesis, 2007.